Characterization of recombinant human kidney diamine oxidase and equine plasma amine oxidase
by Bradley Owen Elmore

A dissertation submitted in partial fulfillment of the requirements for the degree of Doctor of Philosophy m Biochemistry
Montana State University

Abstract:
Human kidney diamine oxidase has been overexpressed as a secreted protein in Drosophila S2 cell culture. This represents the first heterologous overexpression and purification of a catalytically active, recombinant, mammalian copper-containing amine oxidase. To date, the direct examination of mammalian copper-containing amine oxidases has been difficult and limited, especially true for the human enzyme. The availability of large quantities of highly purified enzyme makes it now possible to investigate the spectroscopic, mechanistic, functional and structural properties of this human enzyme at the molecular level. Visible absorption, circular dichroism, electron paramagnetic resonance and resonance Raman spectroscopic results are presented. The recombinant enzyme contains the cofactors 2,4,5-trihydroxyphenylalanine quinone (TPQ) and copper at stoichiometries around 1.1 and 1.5 mol per mol homodimer, respectively. In addition, tightly bound and stoichiometric calcium ions were identified and are proposed to occupy the second metal binding site. Detailed kinetic studies indicate the preferred substrates are, in order, histamine, 1-methylhistamine, agmatine and putrescine. Inhibition by pharmaceutical compounds has been examined, and most notably, pentamidine has been demonstrated to be a competitive inhibitor with an inhibition constant in low nanomolar range. Azide is shown to be a competitive inhibitor against both substrate amine and dioxygen. Equine plasma copper-containing amine oxidase has also been purified from the natural source and characterized.

CHARACTERIZATION OF RECOMBINANT HUMAN KIDNEY DIAMINE OXIDASE AND EQUINE PLASMA AMINE OXIDASE

by

Bradley Owen Elmore

A dissertation submitted in partial fulfillment
of the requirements for the degree

of

Doctor of Philosophy

in

Biochemistry

MONTANA STATE UNIVERSITY
Bozeman, Montana

October 2002

APPROVAL

of a dissertation submitted by

Bradley Owen Elmore

This dissertation has been read by each member of the dissertation committee and has been found to be satisfactory regarding content, English usage, format, citations, bibliographic style, and consistency, and is ready for submission to the College of Graduate Studies.

David M. Dooley — (Signature) — Date 10.25.02

Approved for the Department of Chemistry and Biochemistry

Paul A. Grieco — (Signature) — Date 10-25-02

Approved for the College of Graduate Studies

Bruce R. McLeod — (Signature) — Date 10-29-02

STATEMENT OF PERMISSION TO USE

In presenting this thesis in partial fulfillment of the requirements for a doctoral degree at Montana State University, I agree that the Library shall make it available to borrowers under rules of the Library. I further agree that copying of this dissertation is allowable only for scholarly purposes, consistent with "fair use" as prescribed in the U.S. Copyright Law. Requests for extensive copying or reproduction of this dissertation should be referred to Bell & Howell Information and Learning, 300 North Zeeb Road, Ann Arbor, Michigan 48106, to whom I have granted "the exclusive right to reproduce and distribute my dissertation in and from microform along with the non-exclusive right to reproduce and distribute my abstract in any format in whole or in part."

Signature 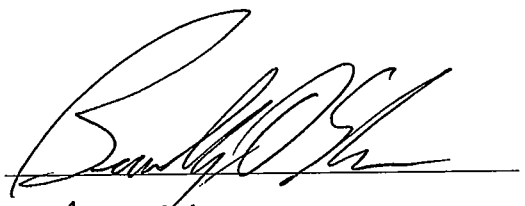

Date October 21, 2002

This thesis is dedicated to Nathan and Joshua Elmore,

who shared in my sacrifice and offered unconditional support, faith and love.

TABLE OF CONTENTS

LIST OF TABLES

Table Page

LIST OF FIGURES

Figure Page

ABSTRACT

Human kidney diamine oxidase has been overexpressed as a secreted protein in *Drosophila* S2 cell culture. This represents the first heterologous overexpression and purification of a catalytically active, recombinant, mammalian copper-containing amine oxidase. To date, the direct examination of mammalian copper-containing amine oxidases has been difficult and limited, especially true for the human enzyme. The availability of large quantities of highly purified enzyme makes it now possible to investigate the spectroscopic, mechanistic, functional and structural properties of this human enzyme at the molecular level. Visible absorption, circular dichroism, electron paramagnetic resonance and resonance Raman spectroscopic results are presented. The recombinant enzyme contains the cofactors 2,4,5-trihydroxyphenylalanine quinone (TPQ) and copper at stoichiometries around 1.1 and 1.5 mol per mol homodimer, respectively. In addition, tightly bound and stoichiometric calcium ions were identified and are proposed to occupy the second metal binding site. Detailed kinetic studies indicate the preferred substrates are, in order, histamine, 1-methylhistamine, agmatine and putrescine. Inhibition by pharmaceutical compounds has been examined, and most notably, pentamidine has been demonstrated to be a competitive inhibitor with an inhibition constant in low nanomolar range. Azide is shown to be a competitive inhibitor against both substrate amine and dioxygen. Equine plasma copper-containing amine oxidase has also been purified from the natural source and characterized.

INTRODUCTION

Post-Translationally Modified Amino Acid Cofactors

Biological systems have developed the means to substantially extend the chemical properties and thus functionality of the twenty common amino acids that make up proteins via chemical modification. A special case is the post-translationally modified amino acids that serve as cofactors in enzyme catalysis and thus supplement the "normal" complement of enzyme cofactors and prosthetic groups, such as NAD(H), flavins, pyridoxal phosphate, Fe-heme groups, metal ions, etc.

This recently discovered group of enzymes requires the post-translational modification of an intrinsic, encoded amino acid residue for catalytic activity. The number of these modified cofactors, currently 19, will likely soon outnumber the naturally occurring amino acids used in protein biosynthesis. This group of enzymes has representatives in every branch of life and includes enzymes of fundamental importance to life on earth. For example, cytochrome c oxidase, the terminal oxidase of the electron transport chain, contains a tyrosine cross-linked to a histidine ligand of Cu_B. Ribulose-1,5-bisphosphate carboxylase (rubisco), responsible for the first step of photosynthetic CO_2 fixation, contains a carbamylated lysine residue that ligates a magnesium ion. A recent review is by Okeley and Van der Donk [1].

A sub-group of post-translationally modified amino acid cofactors is comprised of those that contain a quinone cofactor (Figure 1). TPQ, 2,4-trihydroxyphenylalanine quinone, is the organic tyrosine derived cofactor in the copper containing amine oxidases

(EC 1.4.3.6). LTQ, lysyl tyrosylquinone, is found in the copper containing lysyl oxidases (EC 1.4.3.13), which oxidize peptidyl lysine residues for cross-linking of elastin and collagen in connective tissue. Tryptophan tyrptophylquinone (TTQ), an oxidized cross-link between two tryptophans is present in bacterial methylamine dehydrogenase (EC 1.4.99.3). CTQ, cysteine tryptophyl quinone, is a very recent addition to this group and is formed from the oxidation of a cross-linked cysteine and tryptophan in the bacterial quinohemoprotein amine dehydrogenase.

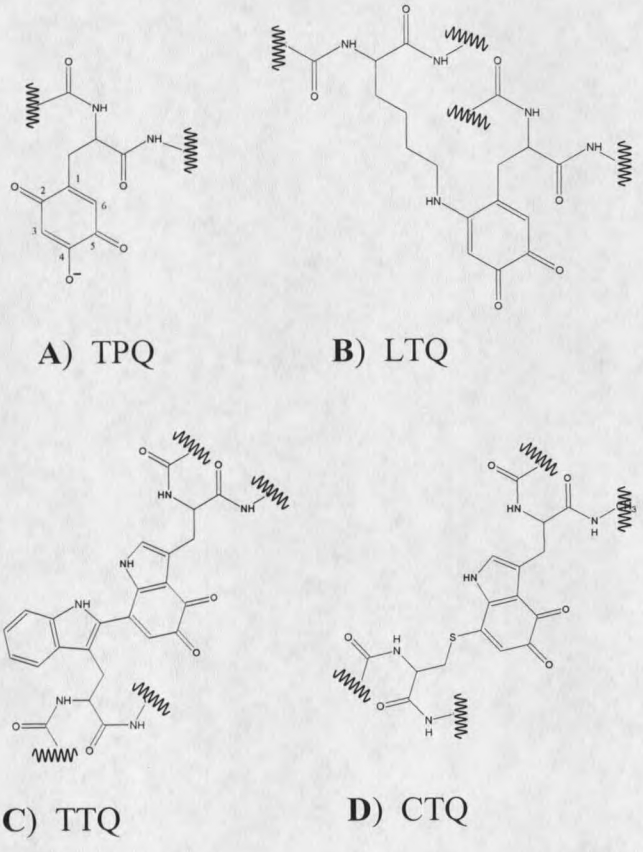

Figure 1. Post-translationally modified quinone cofactors; **A**) 2,4-trihydroxyphenylalanine quinone, TPQ; **B**) lysyl tyrosylquinone, LTQ; **C**) tryptophan tyrphophylquinone, TTQ; **D**) cysteine tryptophyl quinone, CTQ

Copper Containing Amine Oxidases

The TPQ containing enzymes, copper containing amine oxidases (CAOs) are the focus of this thesis. There is another distinct class of enzymes referred to as amine oxidase, monoamine oxidase, tyramine oxidase, adrenalin oxidase, or polyamine oxidase. This latter group, EC 1.4.3.4, contains a flavin cofactor and will not be discussed herein.

CAO's are homodimers, generally ranging in size from 140 to 200 kDa, with one active site found in each monomer [2]. Each active site contains two cofactors: 1) a single Type II copper ion, and 2) TPQ. The quinone cofactor is derived from the post-translational modification of an invariant tyrosine residue [3]. TPQ has been shown to be produced in a novel, self-processing reaction requiring only copper and dioxygen [4-7]. CAOs are unique in that they are homodimeric, contain one organic and one inorganic cofactor in each of two active sites, and the organic cofactor is a quinone from the autocatalytic oxidation of an intrinsic tyrosine.

TPQ containing enzymes are pink in color, with a broad absorption feature around 480 nm attributed to the quinone cofactor. In the active enzyme, TPQ is an oxoanion [8]. Resonance Raman spectra indicate the charge is delocalized over the C2 and C4 oxygens (Figure 2) [9]. Differences in the TPQ λ_{max} values among CAOs from different sources are thought to reflect the degree of charge localization [10].

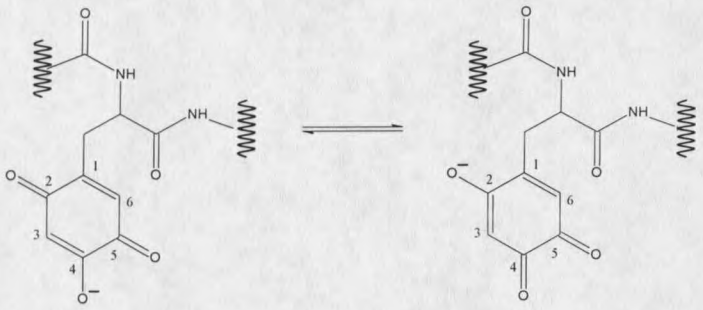

Figure 2. TPQ resonance structures

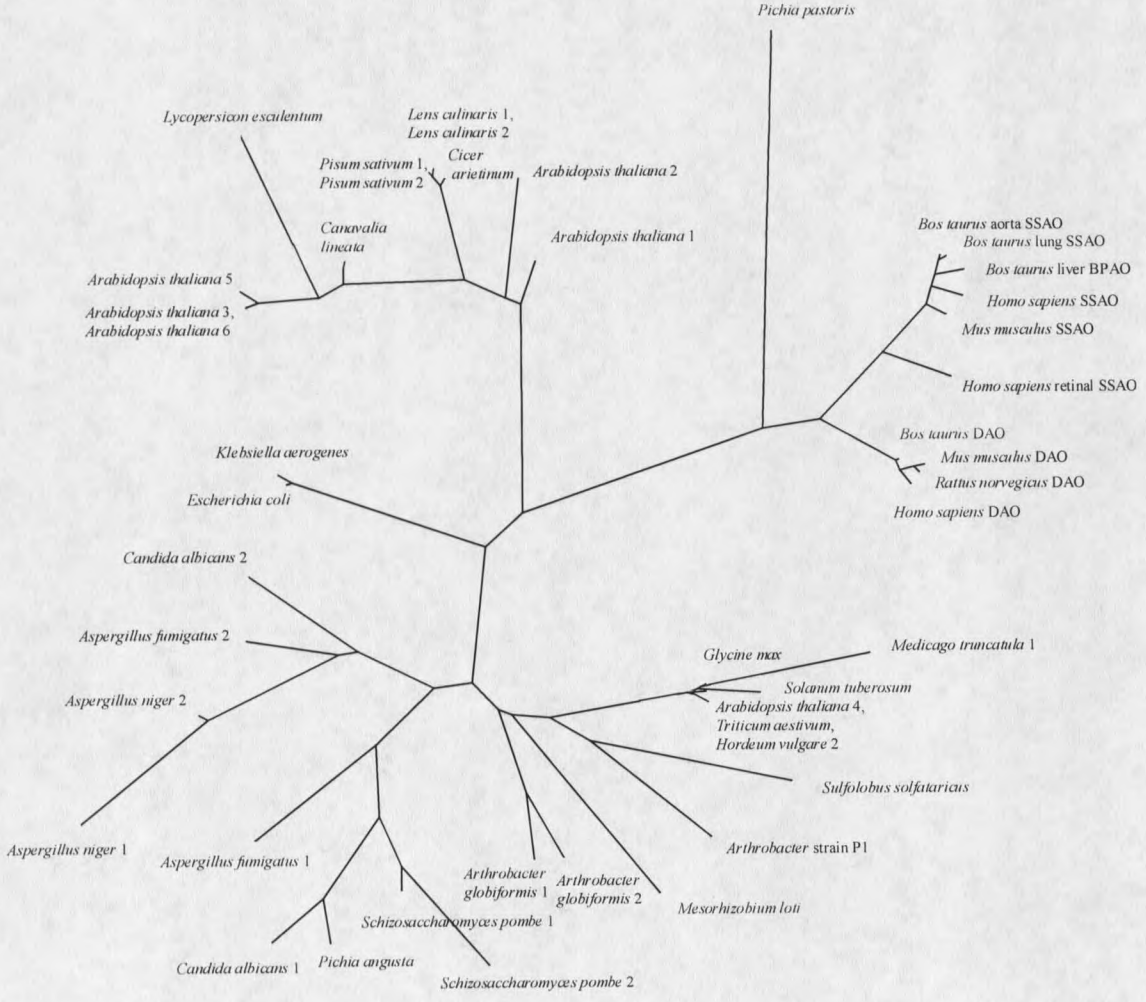

Figure 3. Phylogenetic tree for the copper amine oxidases

CAOs are widespread in nature, having been described from gram-positive and gram-negative bacteria, yeast and fungi, plants and animals [2]. Recently the gene encoding a copper amine oxidase has been sequenced from the archaea *Solfolobus solfataricus*. Figure 3 shows a phylogenetic tree constructed for the family of copper containing amine oxidases, see Appendix B for details. An alignment of the amino acid sequences for all CAOs sequenced to date is given in Appendix A.

Structure

The structures of four copper amine oxidases have been solved by x-ray crystallography: two are bacterial (*Escherichia coli* and *Arthrobacter globiformis*), one is from the yeast *Hansenula polymorpha* (formally classified as *Pichia angusta*), and one is from pea seedling (*Pisum sativum*) [11-14]. Collectively these four enzymes exhibit considerable structural homology, although primary sequence identity is less than 40% between any two. The enzymes are "mushroom" shaped with an extensive intersubunit contact, including a pair of "arms" extending from each subunit to embrace the other. Figure 4 shows the ribbon structure of the *Eschericia coli* copper amine oxidase (ECAO). Each monomer is comprised of four domains. The N-terminal domain (D1) forms the "stalk" portion of the "mushroom" and is not present in all copper amine oxidases. A large (440-amino acid) β-sandwich C-terminal domain contains the active site and forms the majority of the dimer interface. Domains D2 and D3 have remarkably similar folds, an α-helix and a four-stranded antiparallel β-sheet. A channel for substrate access and product exit lies between domains D3 and D4.

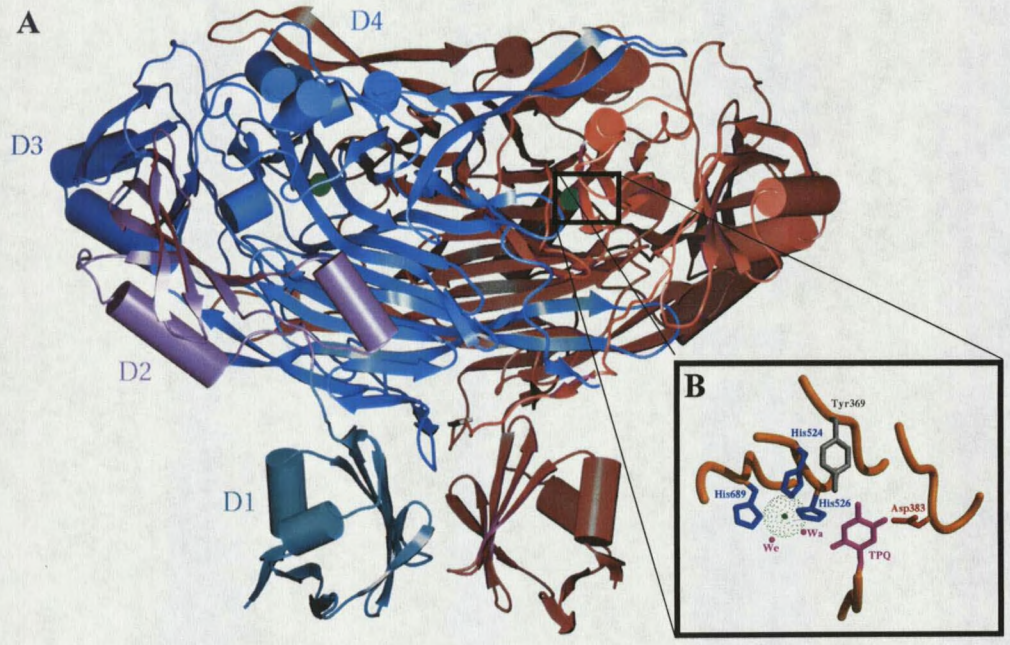

Figure 4. Structure of the ECAO homodimer. One monomer is red, and the other monomer has individual domains colored different shades of blue and indicated by D1-D4. Copper ions are shown as green spheres. **B**, Schematic of ECAO active site, showing the copper ion and TPQ cofactors. The water axial and equatorial ligands to the copper ion are labeled Wa and We, respectively. (from Wilmot, C.M., et al. *Science* **1999**, *286*, 1724)

The crystallographically determined structures confirm the copper coordination environment as predicted from spectroscopy [15-17]. The active-site copper ion is coordinated in a distorted square pyramidal geometry by three conserved histidine residues and two water molecules, one axial and the other equatorial. Also, the quinone cofactor is in close proximity to the copper ion and can be observed in different conformations, indicative of inherent side-chain flexibility. Figure 5 shows the view of important features from active site of the pea seedling CAO (PSAO).

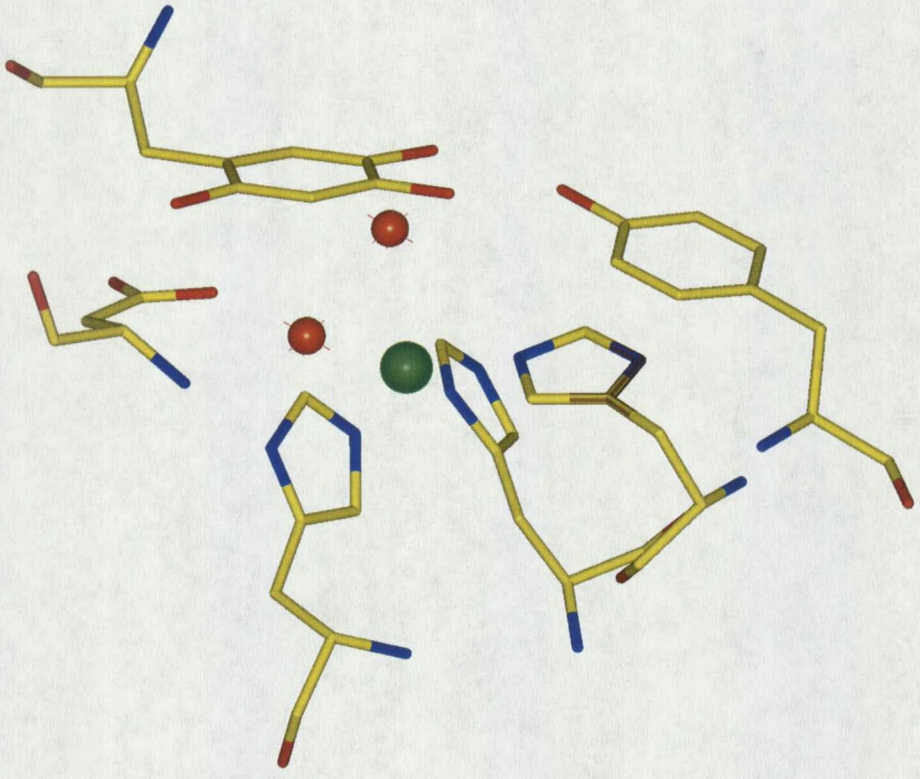

Figure 5. The active site of PSAO. The copper ion is represented by a green sphere, water molecules by red spheres. The three hisidine and the axial water ligands to copper are shown. TPQ is at the top of the figure, and an invariant tyrosine residue that hydrogen bonds to TPQ is to the right. On the left side is an invariant aspartate that serves as a base during catalysis.

Mechanism

The copper-containing amine oxidases catalyze the two-electron oxidative deamination of primary amines to the corresponding aldehyde, using dioxygen as the oxidant, with the concomitant production of ammonia and hydrogen peroxide. Catalysis proceeds through a Bi Ter Ping Pong mechanism divided into two half-reactions:

$$E_{ox} + RCH_2NH_2 \leftrightarrows E\text{-}RCH_2NH_2 \rightarrow E_{red} + RCHO$$

$$E_{red} + O_2 \rightarrow E_{ox} + H_2O_2 + NH_3$$

The first half reaction is conventionally termed the "reductive half reaction". Substrate amine is oxidized to an aldehyde and the TPQ is reduced by two electrons. The "oxidative half reaction" uses molecular oxygen to regenerate the oxidized form of TPQ. Recent reviews are found in references [10] and [18].

Figure 6 diagrams the enzyme active site and steps in the catalytic cycle. Detailed kinetic studies have elucidated many of the details of the reductive half reaction. Substrate combines with the oxidized, resting form of the enzyme (A, Figure 6) to form a covalent substrate Schiff base adduct at C-5 of TPQ (B, Figure 6). Proton abstraction from the α carbon of substrate, using a conserved active site aspartate residue, yields a product Schiff base adduct and reduced TPQ (C, Figure 6). Proton abstraction has been shown to at least partially contribute to the rate-determining step in a few mammalian enzymes. Product aldehyde is subsequently released by hydrolysis, leaving the aminoquinol form of TPQ.

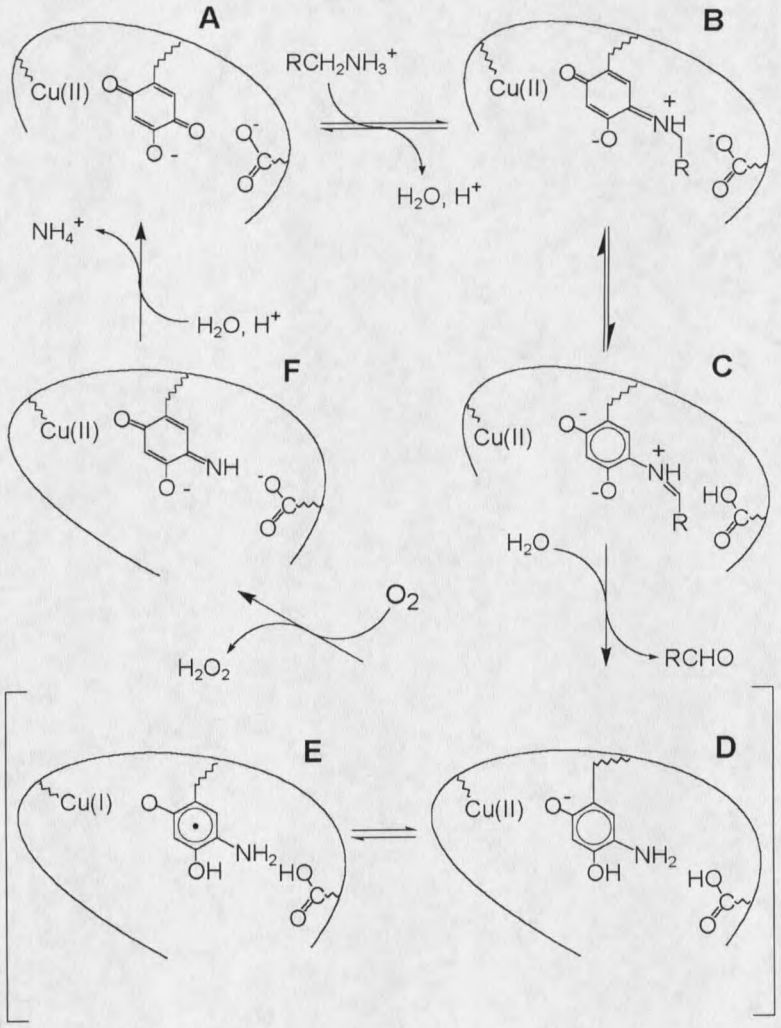

Figure 6. Proposed reaction mechanism for the oxidation of amines by copper-containing amine oxidases.
The oxidized, resting enzyme (**A**) combines with amine substrate to give a substrate Schiff base (**B**). Proton abstraction by the conserved active-site aspartate from the substrate's α-carbon results in a product Schiff base and reduced TPQ (**C**). Product aldehyde is release by hydrolysis, leaving the aminoquinol form of the enzyme (**D**). This Cu(II)-aminoquinol is in equilibrium with a Cu(I)-aminosemiquinone radical form(**E**). The enzyme is then oxidized, with dioxygen serving as the electron acceptor. Oxidation proceeds through a postulated aminoquinone intermediate (**F**), liberates ammonium and regenerating the resting enzyme (**A**).

The oxidative half reaction is less well understood. The substrate-reduced enzyme has been shown to be an equilibrium mixture of the Cu(II)-aminoquinol and Cu(I)-aminosemiquinone radical forms(D, E in Figure 6) under anaerobic conditions, and the Cu(I)-aminosemiquinone species would be expected to readily react with dioxygen [19]. A no bligatory m echanistic r ole for C u(I) has n ot b een e stablished, a nd a v iable alternative utilizing only the Cu(II) oxidation state has recently been proposed [20]. Dioxygen is reduced to peroxide to give a postulated iminoquinone intermediate (F in Figure 6), and hydrolysis regenerates the oxidized quinone.

The mechanism of dioxygen reduction remains a central question; how does the enzyme activate dioxygen for the two-electron reduction to hydrogen peroxide? The anaerobic substrate-reduced enzyme has been shown by EPR spectroscopy to be an equilibrium mixture of Cu(II)–aminoquinol and Cu(I)–semiquinone radical forms, where Cu(I) would be anticipated to reduce dioxygen [19]. The formation of the Cu(I)–semiquinone has been shown to be kinetically competent in bacterial and plant enzymes [21]. Furthermore, considerable chemical precedence exists for the binding and activation of oxygen by copper(I) ions [22-25].

Recent solvent isotope effect, O-18 isotope effect, and solvent viscosity effect work using bovine serum amine oxidase indicates that the first-electron transfer to dioxygen, and not oxygen binding, is the rate-determining step for the oxidative half-reaction [20]. Because Su and Klinman expected a Cu(I) reduction of dioxygen to be relatively fast, they proposed that dioxygen is prebound, and the rate-limiting, first-electron transfer (to produce superoxide) occurs at a site other than the Cu(I) center. A

hydrophobic pocket in the *Hansenula polymorpha* CAO active site was identified and suggested to be the site of dioxygen binding and initial reduction. The second-electron transfer, resulting in the reduction of superoxide to peroxide, could either occur in the hydrophobic pocket or after superoxide binds to Cu(II). More recent work of Mills and Klinman using the cobalt-substituted *H. polymorpha* enzyme lends support to a nonredox role for copper in TPQ reoxidation [26].

Mammalian Copper Amine Oxidases

Three general classes of CAOs have been described from mammalian sources; unfortunately, the nomenclature in the literature is frequently confusing. One type of amine oxidase is found tightly associated with tissues, is active against monoamine substrates, and is commonly designated semicarbazide-sensitive amine oxidase (SSAO). It must be noted that all CAOs are inhibited by semicarbazide, so the designation of the tissue-associated amine oxidases as SSAOs is simply a convention. Sequence analysis has recently revealed these tissue-bound enzymes possess a single putative N-terminal transmembrane helix [27]. Another variety of CAO is soluble, found in blood plasma, and is active against a wide range of monoamines, diamines, and aromatic amines. These enzymes are generally termed plasma amine oxidases, serum amine oxidases, or benzylamine oxidases, and are thought to be synthesized in the liver [28]. The third type of mammalian CAO is also soluble, but displays distinct substrate specificity for diamines. This group is therefore termed diamine oxidases (DAOs). These are also distinct in sequence homology from the soluble plasma and the membrane-bound CAOs

[29,30]. The amino acid alignment for available mammalian copper amine oxidases is given in Appendix A.

Barbry and coworkers identified the first complete nucleotide sequence for a mammalian copper-containing diamine oxidase, that of the human kidney (previously misidentified as a protein associated with the amiloride-sensitive Na^+ channel) [31]. The translated cDNA sequence encodes a 751 amino acid polypeptide with a predicted 19 amino acid signal sequence for the classical secretory pathway. N-terminal sequencing of human DAO purified from kidney and placenta demonstrated the mature protein lacked these residues, confirming the predicted signal cleavage site. The amino acid sequence contains the copper amine oxidase consensus sequence, T/SXXNYD/EY/N (residues 457-463), in which the first tyrosine residue is modified to TPQ in the mature enzyme. A heparin-binding consensus sequence, RFKRRLPK, was also recognized (residues 569 - 576).

One unanticipated finding in the crystal structures of the *E. coli* and pea seedling CAOs was the identification of an additional metal-binding site in each subunit, modeled as being occupied by a calcium and a manganese ion, respectively. Three aspartate carboxylates, two peptide carbonyl oxygens and one water molecule coordinate this second metal ion. These aspartate ligands are absolutely conserved in all ten sequenced mammalian CAOs, and in more than 50% of all available sequences representing bacteria, fungi, plants and animals. The second-metal site and the inferred location of the heparin binding sequence are both on the solvent exposed upper surface of the "mushroom cap" [14].

Research Goals

Although considerable details for the copper-containing amine oxidases structure and mechanism have been elucidated, many questions remain, particularly with respect to the mammalian enzymes. One major goal of this research project is to obtain large quantities of highly purified mammalian copper-containing amine oxidases that are amendable to detailed and comprehensive spectroscopic, kinetic, biochemical and structural studies. This work describes the development of a heterologous overexpression system for the recombinant human kidney diamine oxidase (rhKDAO). In addition highly purified equine plasma amine oxidase has been obtained from the natural source.

One outstanding and fundamental aspect of the mammalian copper-containing amine oxidases is that the physiological functions have not yet been unambiguously defined. Examination of the substrate specificities and catalytic kinetics for the recombinant enzyme, using biogenic and exogenous amines, has provided important insight that can be used to infer *in vivo* details. The biogenic amines histamine, 1-methylhistamine, agmatine and putrescine have proven to be excellent substrate for the recombinant enzyme. Investigations into rhKDAO interactions with pharmaceutical compounds has given some striking results that may facilitate the rational design of highly specific diamine oxidase inhibitor and potentially drugs with reduced side effects and toxicity. Furthermore, the overexpression of the recombinant enzyme will facilitate experiments designed to investigate the molecular details of copper amine oxidase

activity. One such experiment, the interaction of the small anion azide, is given here and provides exciting data specific for the controversial oxidative half reaction.

The determination of a mammalian crystal structure from a copper-containing amine oxidase would represent a major breakthrough. Attempts to obtain good quality crystals were performed using the equine plasma amine oxidase. Additional crystallization trials with both of the mammalian enzymes utilized in this work remain a high priority. While a crystal structure is not imminent, when available a structure would provide structural details that are key to understanding features such as the control of substrate and inhibitor recognition and insight into the chemical mechanism.

EXPRESSION, PURIFICATION AND CHARACTERIZATION OF RECOMBINANT HUMAN KIDNEY DIAMINE OXIDASE

Introduction

The detailed characterization and direct examination of mammalian copper amine oxidases has been greatly hindered by the difficulty in obtaining the quantities of highly purified enzyme required. Purifications from natural sources are long and tedious and give highly variable purities and activities. Many researchers had no choice but to use crude preparations, sometimes tissue homogenates. Prior to the results given herein, there has been no reliable overexpression system for a copper amine oxidase from any multicellular organism.

To further the extent and depth of knowledge about diamine oxidase, an enzyme implicated in fundamental and critically important biological processes, it is vital to have a readily-available source of homogenous protein. Our approach has been to heterologously overexpress the human enzyme using a eukaryotic host, *Drosophila* S2 insect cell culture. This expression system was chosen for its relative ease in culturing, potential for high expression levels, and apparent lack of an endogenous copper-containing amine oxidase. We report herein the heterologous overexpression and purification of human kidney diamine oxidase, the first successful overexpression of any mammalian copper-containing amine oxidase. Furthermore, high levels of expression and a developed purification protocol give the large quantities of highly-purified enzyme required for detailed investigation of molecular properties.

In this chapter, the overexpression system and purification protocol are described. Initial characterization of the recombinant enzyme includes molecular weight determination, cofactor quantification, and measurement of its visible absorption, circular dichroism, electron paramagnetic resonance, and resonance Raman spectra. The nature and quantification of the organic TPQ cofactor and metal analysis are discussed along with elementary biochemical characterization of the recombinant enzyme. Additionally, human tissue-specific expression data is presented.

Experimental Procedures

Construction of cell line

The initial molecular biology, *Drosophila* S2 transfection and expression were performed by Dr. John Bollinger (MSU).

The coding sequence for mature human kidney diamine oxidase was amplified by PCR from a cDNA clone (kindly provided by Dr. Barbry, Institut de Pharmacologie Moléculaire et Cellulaire, France) using Vent DNA Polymerase and appropriate primer adapters. The forward primer (5′-GTGAGATCTCCGGGGACTCTGCCC) replaced the N-terminal codons for glutamic acid and proline of mature kidney diamine oxidase with the codon for arginine and introduced a *Bgl*II site. The reverse primer (5′-CCGGAATTCACGATGCCGGCCCTGGGCTGGGCC) introduced an *Eco*RI site just downstream from the native stop codon. PCR product and the expression vector pMT/BiP/V5-His A (Invitrogen) were digested with *Bgl*II and *Eco*RI, agarose gel

purified, recovered using Prep-A-Gene (Bio-Rad) and ligated with T4 DNA ligase. The 5′ end of the resulting construct was confirmed by DNA sequencing (Silver Sequence, Promega) through the fusion site to an internal *Bst*II site, 350 base pairs into the coding sequence. The remainder of the coding sequence was swapped with a *Bst*II and *Eco*RI fragment from the cDNA clone to generate the expression vector pMTDAO. All DNA manipulations used enzymes from New England Biolabs. Constructs were maintained in *E. coli* strain TOP10 and purified using either Perfect Prep (5Prime3Prime) or Quantum Prep (Bio-Rad).

Transfection and cell culturing procedures were those outlined in the *Drosophila* Expression System Manual (Invitrogen), except as noted. Plasmids pMTDAO and the selection vector pCoHYGRO were cotransfected into *Drosophila* Schneider 2 (S2) cells at a ratio of 19:1 (μg) using the Calcium Phosphate Transfection Kit (Invitrogen). Selection for the stably transfected subpopulation used 500 μg/mL hygromycin B (Roche Molecular Biochemicals). The resulting polyclonal cell line was adapted to and maintained in a serum-free medium (Ex-Cell 400, JRH Biosciences) supplemented with 300 μg/mL hygromycin B at 27 °C.

Expression

The transfected cell line was expanded from a 5 mL culture in a 25 cm^2 tissue culture flask to a single 130 mL culture in a 250 mL spinner flask. When the spinner culture reached a density of 1×10^7 cells/mL, 25 mL of the culture was added to each of four 500 mL baffled shake flasks (Bellco Glass) containing 150 mL serum-free medium.

Flasks were incubated in a gyrotary water bath at 110 rpm and 27 °C for about 24 hours. At a density of 5 x 10^6 cells/mL, expression was induced by addition of copper sulfate to a final concentration of 500 μM, and incubation was then continued for 48 hours. Nontransfected *Drosophila* S2 cells and the uninduced expression cell line were used as negative controls.

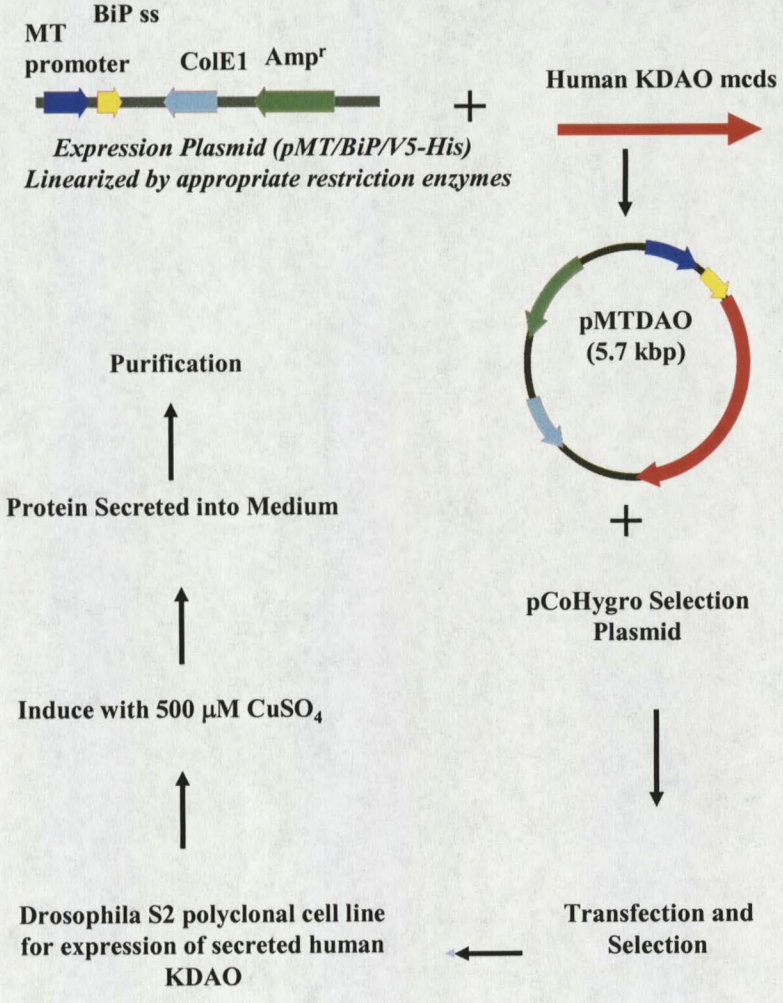

Figure 7: Schematic of the expression of hKDAO in *Drosophila* S2 cells

Purification

Cultures were harvested and cells spun out by centrifugation for 2 minutes at 1000 x *g*. The supernatant was spun for 10 minutes at 10000 x *g* to remove particulates and then loaded on a 5mL HiTrap Heparin HP column (Amersham Pharmacia Biotech) using a peristaltic pump. The column was then washed with 100 mM potassium phosphate buffer, pH 7.2, until A_{280} of the flow through reached zero, and bound protein was eluted with 100 mM potassium phosphate with 1 M sodium chloride, pH 7.2. The eluant was extensively dialyzed against 100 mM potassium phosphate, pH 7.2 and then loaded on Macro-Prep Ceramic Hydroxyapatite (Type I, 40 μm particle size, Bio-Rad) in a HR 10/10 column using a FPLC system (Amersham Pharmacia Biotech). Buffers for the ceramic hydroxyapatite column were 100 mM potassium phosphate, pH 7.2 (Buffer A) and 400 mM potassium phosphate, pH 7.2 (Buffer B). Protein fractions were eluted with a two column volume wash at 25% Buffer B, a single column volume wash at 35% Buffer B, and a two column volume linear gradient from 35% to 100% Buffer B. The most active fractions were pooled and concentrated in a 50 mL centrifugal concentrator (Millipore) before being run over a 1.6 x 100 cm Ultrogel AcA 34 (BioSepra) gel filtration column equilibrated in 100 mM potassium phosphate, pH 7.2. SDS/PAGE and IEF gels were by a PhastSystem (Pharmacia). Substantial absorbance at 280 nm in the culture media necessitated that initial protein concentration be determination by the Bradford protein assay (Bio-Rad) with bovine serum albumin standards. Subsequent protein concentrations were determined spectrophotometrically by absorbance at 280 nm using the predicted extinction coefficient for the mature, recombinant enzyme of 280.5

$mM^{-1}cm^{-1}$. [32] The extinction coefficient at 280 nm was later determined by magnetic circular dichroism and calculated as 297.6 $mM^{-1}cm^{-1}$ (data not shown) [33].

General Characterization

Amine oxidase activity was measured at 37 °C in a stirred, thermostatted cuvette using a coupled assay with putrescine (dihydrochloride, Sigma) as the substrate. Standard activity assays used 30 U horseradish peroxidase (Sigma), 10 mM putrescine, and 2 mM ABTS (2,2'-Azino-bis(3-ethylbenzothiazoline-6-sulfonic acid) in 100 mM potassium phosphate, pH 7.2, in a final volume of 2 mL. Reaction progress was followed spectrophotometrically by monitoring the change in absorbance at 414 nm (ε = 24.6 $mM^{-1}cm^{-1}$) [34]. Activities measured by dioxygen depletion using an Instech oxygen electrode and chamber were in close agreement to those measured by the coupled assay (data not shown).

UV and visible absorption data were acquired with either a Hewlett-Packard 8452A or 8453 diode-array spectrophotometer. CD spectra were obtained with a Jasco J-710 spectropolarimeter. Titrations with phenylhydrazine (HCl, Sigma) were used to quantify TPQ in the purified recombinant enzyme [35]. One mL of 10-20 μM protein in 100 mM potassium phosphate buffer was titrated with 2 μL aliquots of fresh, anaerobically-prepared phenylhdrazine (~775 μM) at room temperature. Spectral changes were monitored and recorded after the absorbance at 445 nm reached a constant value following each addition (10 - 45 minutes). The derivatized enzyme was subsequently concentrated in a Microcon 30 (Millipore) with buffer exchange to remove

unreacted phenylhydrazine. The concentrated phenylhydrazine-derivatized enzyme was then used for resonance Raman spectroscopy on a Spex Triplemate spectrometer with a CCD detector, with excitation by a Coherent argon-ion laser. EPR spectra were recorded on a Bruker 220D SRC interfaced with a personal computer. Simulation of EPR spectra used the EPR XOP for Igor Pro by John Boswell (Oregon Graduate Institute), an adaptation of "Program QPOW by Nilges and Belford [36-38]. Copper, zinc, calcium and magnesium analysis were performed by ICP emission spectroscopy (Little Bear Laboratories, Inc., Golden, CO), or copper analysis by flame atomic absorption spectroscopy using a Buck Scientific Model 210 VGP. Metal-free buffer was prepared by passage over Chelex-100 (Bio-Rad) and by using plasticware treated with 0.1 M EDTA solution. Analytical ultracentrifugation and ES/MS services were kindly provided by Andy Baron and Alison Ashcroft, respectively, at the University of Leeds, Leeds, UK.

Tissue-Specific Gene Expression

A Multiple Tissue Expression Array (Clontech) was used to determine the human, tissue-specific expression profile of human diamine oxidase. The manufacturer's instructions were followed for generating ^{35}P-labelled cDNA probes by random primer labeling, hybridization and autoradiography. This experiment was performed by Dr. John Bollinger (MSU).

Results

Expression and purification

The expression vector pMTDAO contains the coding sequence for mature human kidney diamine (hKDAO) oxidase fused to *Drosophila* BiP signal sequence for secretion from *Drosophila* S2 cell culture. Expression is under the control of the *Drosophila* metallothionein promoter and induced by addition of copper sulfate to 500 μM. Mature recombinant human kidney diamine oxidase (rhKDAO) primary sequence, as deduced from the DNA sequence, differs from that of the natural protein in only the replacement of the N-terminal glutamic acid and proline with an arginine residue.

Culture medium was harvested 48 hours post-induction at a cell density of 1.45 x 10^7 cells per mL. Cells were greater than 99% viable as determined by trypan blue staining and exhibited normal morphology. No amine oxidase activity was detected in either the uninduced expression cell line or in the parental S2 cell line.

The recombinant enzyme is readily purified by heparin affinity chromatography, ceramic hydroxyapatite chromatography and gel filtration; the summary of a representative purification is given in Table 1. Total enzymatic activity increases during the protocol and likely reflects the loss of an inhibiting substance (of either the amine oxidase or the coupled assay) that is present in the growth medium. The purified protein is estimated at greater than 98% homogenous by SDS/PAGE, and the highest specific activity obtained from any purification was 1.25 I.U./mg.

Purified rhKDAO is stable for several months when stored on ice. However, freezing the enzyme at –20 °C gives a significant drop in specific activity; thawed enzyme has about 40% the specific activity of that before freezing. Thawed protein can recover 85% of the original specific activity after storing on ice for ten days. Bieganski and coworkers have previously noted a 90% loss in activity with natural human diamine oxidase when stored at -20 °C [39].

Step	Total Volume (mL)	Total Protein (mg)	Total Activity (I.U.)	Specific Activity (I.U./mg)	Purification Factor
Culture medium	630	117	7.3	0.063	1
Hi-Trap Heparin	13.5	41	12.5	0.30	4.8
Ceramic hydroxyapatite	44	14	13.0	0.93	14.8
Ultrogel AcA34	0.74	12	12.7	1.1	16.7

Table 1. Purification of recombinant human kidney diamine oxidase

Electrophoresis and analytical ultracentrifugation

Isoelectric focusing acrylamide gel electrophoresis gave an estimated pI of 6.2, and only a single protein band was observed. A pI of 6.7 is predicted from the primary sequence of rhKDAO [40]. Previous investigations reported isoelectric points of 6.0 and 7.1 for the natural human DAO [41-43].

SDS/PAGE of the purified enzyme gives a single protein band with an apparent molecular weight of 94 kDa (Figure 8), although the primary sequence of rhKDAO predicts 83.4 kDa for the mature monomer. No corresponding band is detected in

negative controls. The ~10 kDa discrepancy between the predicted and observed molecular weights suggests the expressed protein is substantially glycosylated (vide infra). Literature values for the apparent molecular weight of the natural human DAO have been reported as 70, 90 and 105 kDa by SDS/PAGE [44,45]. As evident in Figure 8, the recombinant protein band represents the major protein in harvested media.

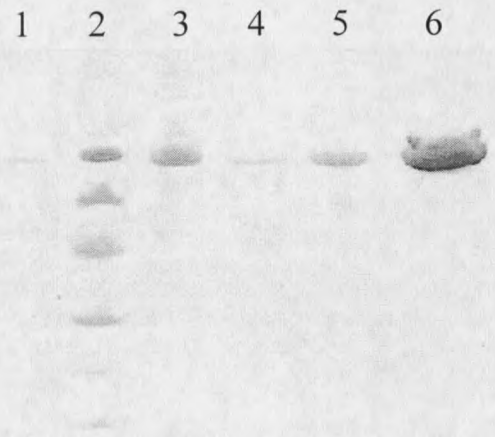

Figure 8. SDS/PAGE showing purification of recombinant human kidney diamine oxidase.
1) Harvested *Drosophila* S2 media diluted 1:1 with gel loading buffer;
2) Molecular weight standards: 94, 67, 43, 30, 20.1 and 14.4 kDa;
3) Protein after Hi-Trap Heparin affinity column, 3.6 μg;
4) Following ceramic hydroxyapatite chromatography;
5) Purified protein after gel filtration chromatography, 2.4 μ;
6) 9.6 μg of purified rhKDAO. The distorted band is a consequence of the severe overloading of the gel, however, this lane demonstrates the high degree of purity for the recombinant enzyme.

Several attempts to estimate the native molecular weight by acrylamide gel electrophoresis were unsuccessful. Gel filtration on a calibrated AcA 34 Ultrogel column gave an apparent molecular weight of 113 kDa, unrealistically low for the homodimer (data not shown). Interestingly, Crabbe et al. reported native molecular weights for the purified human placental DAO as 70 kDa by Sephadex G-200 gel filtration and 69.5 kDa by polyacrylamide gel electrophoresis. However, sedimentation equilibrium ultracentrifugation data in the same work indicated a native molecular weight of 235 kDa [44]. Baylin and Margolis reported the native molecular weight of human pregnancy plasma DAO as close to 200 kDa, as determined with Sephadex G-200 [46].

Sedimentation equilibrium ultracentrifugation of rhKDAO gave an average apparent molecular weight of 210 kDa (five runs with two protein concentrations at two speeds, data not shown). Curvature of the A_{280} versus radius plot suggests the recombinant enzyme is in reversible equilibrium between dimers and higher order complexes. The data could equally fit dimer-tetramer, dimer-hexamer or dimer-octamer models, with an association constant of 1.2 A_{280}^{-1} for the dimer-tetramer model.

Sedimentation velocity ultracentrifugation gave a sedimentation coefficient of 10 S and a diffusion coefficient of 4.4 Ficks (two runs, data not shown). The apparent molecular weight calculated by the Svedberg equation is 200 kDa. Both sedimentation velocity runs indicated a small shoulder of faster moving material, consistent with a very small amount of higher-order protein association.

Copper, calcium and TPQ

Copper, zinc, calcium and magnesium content in the recombinant enzyme were investigated using either ICP emission spectroscopy or flame atomic absorption. Table 2 shows the results from three different enzyme preparations. The data suggest a mixture of copper and zinc occupying the active sites in the recombinant enzyme; the sum of copper and zinc approaches 2 mol per mol dimeric enzyme. In contrast, purified mammalian copper amine oxidases, as well as those from other organisms, are most often characterized as having two copper ions per dimer [2]. Our results indicate a correlation between copper content and specific activity for the recombinant enzyme; not surprisingly, samples with higher copper content correspond to an increased specific activity.

SpecificActivity (IU/mg)	Cu	Zn	Ca	Mg	TPQ
0.85	1.03	0.79	1.84	0.91	0.72
1.21	1.42[a]	N.D.[b]	N.D.	N.D.	1.04
1.25	1.48	0.40	3.20	0.0	1.08

Table 2. Metal ion and TPQ stoichiometry for recombinant human kidney diamine oxidase as isolated from three enzyme purifications. Metal ion and TPQ values reported as mol per mole dimeric enzyme.
[a] Value determined by flame atomic absorption spectroscopy; all other metal ion quantifications were by ICP emission spectroscopy.
[b] Not determined

Metal analysis and the lack of manganese signal in EPR spectra (Figure 9) strongly suggest calcium occupies the putative second metal site in recombinant human

kidney diamine oxidase. Purified enzyme was dialyzed either against metal-free 100 mM potassium phosphate buffer alone or against three changes of two liters metal-free 100 mM potassium phosphate, 2 mM EDTA, pH 7.2 followed by extensive dialysis against metal-free phosphate buffer. The sample dialyzed against buffer alone was found by ICP emission spectroscopy to contain 2.37 moles calcium and 0.17 moles magnesium per mole of dimeric protein. Whereas the sample treated with EDTA contained 2.16 moles calcium per homodimer, and magnesium levels were below the detection limit of the instrument.

Figure 9 shows the X-band EPR spectra of Cu(II) in purified rhKDAO. The simulated spectrum was kindly provided by Dr. Melanie Rogers (MSU). EPR parameters are derived from simulated spectra ($g_{\perp} = 2.04$, $g_{\parallel} = 2.265$, $A_{\parallel} = 185$ G) and are consistent with published values for CAOs from various sources [2]. Crabbe et al. reported a $g_{\perp}$ value of 2.05 from Q-band EPR spectra of purified human placental diamine oxidase, however, the presence of manganese prevented the determination of other copper parameters. Manganese was not removed by passing the protein over a Chelex 100 column, leading those investigators to conclude the human placental diamine oxidase was a Cu(II)-Mn(II) metalloprotein, with an apparent stoichiometry of 2.0 mol copper and 2.4 mol manganese per mol enzyme dimer [43]. The lack of a characteristic six-line Mn(II) signal in our spectra is convincing evidence against any manganese associated with the recombinant enzyme.

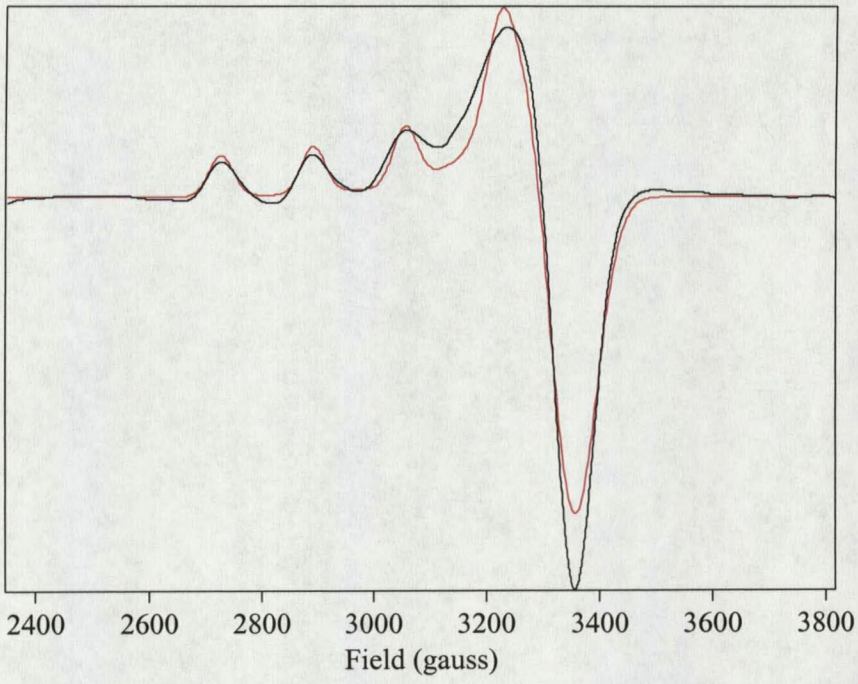

Figure 9. X-band EPR of rhKDAO. Enzyme at ~200 μM in 100 m potassium phosphate buffer (upper spectra). The simulated spectra is shown with $g_{\perp} = 2.04$, $g_{\parallel} = 2.265$ and $A_{\parallel} = 185$ G . Experimental conditions: 77 K, 9.425 GHz, 0.796 mW, 20 G modulation amplitude.

Purified protein is peach-colored with a broad visible absorption band having a λ_{max} at 470 nm (Figure 10). This spectral feature is associated with the TPQ and gives copper amine oxidases their recognizable color. The shoulder in the absorption spectra at 400 nm is an unidentified feature, perhaps due to a modified (possibly incompletely processed) form of the cofactor. The CD spectrum shown in Figure 11 exhibits a negative band around 470 nm that is attributed to TPQ and a negative band around 800 nm from a Cu(II) d-d transition. These electronic transitions are consistent with other CAOs [2], and is consistent with a tetragonal Cu(II) complex with N,O donors.

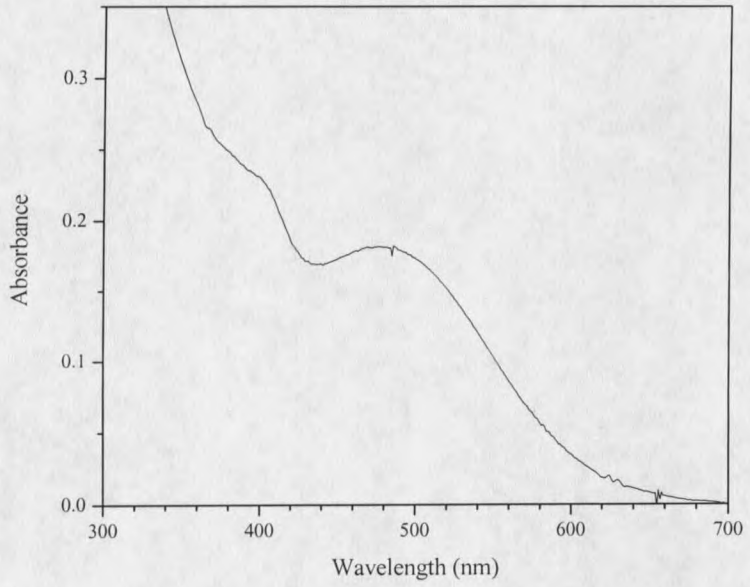

Figure 10. Absorption spectra of the purified recombinant human kidney diamine oxidase, 16.4 mg/mL enzyme in 100 mM potassium phosphate buffer, pH 7.2.

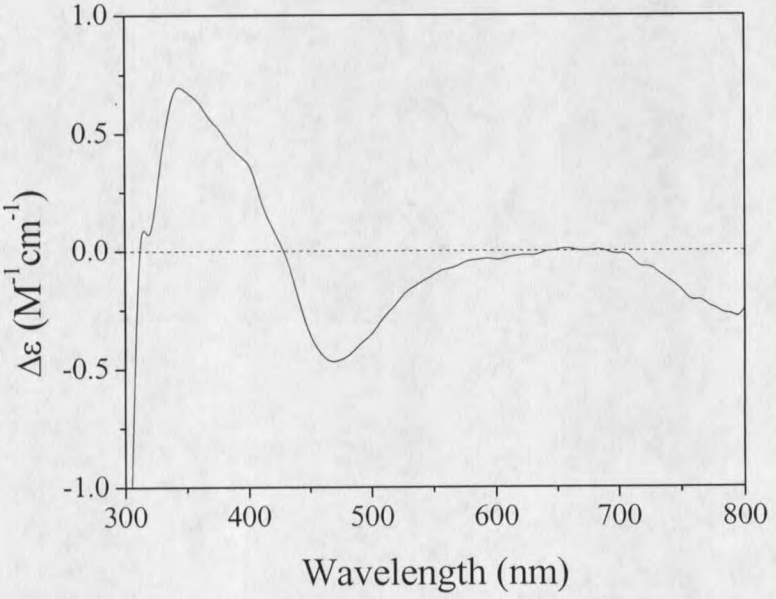

Figure 11. Circular dichroism spectra of rhKDAO. Experimental conditions: 32 μM protein in 100 mM potassium phosphate buffer, pH 7.2, 1 nm resolution, 20 mdeg sensitivity, 1 sec response, 500 μm slit, 5 accumulations.

Copper amine oxidases and the carbonyl reagent phenylhydrazine react to give a characteristic, yellow phenylhydrazone adduct that is commonly used to identify and quantify the TPQ cofactor [2]. Recombinant enzyme was titrated with phenylhydrazine and spectra were recorded after each addition when no further change in absorbance at 442 nm was noted. A typical titration demonstrating the formation of the intensely colored covalent adduct is shown Figure 12 and the results of TPQ quantification for three individual enzyme preparations are shown in Table 2. As described above for copper, the quantified organic cofactor correlates with specific activity.

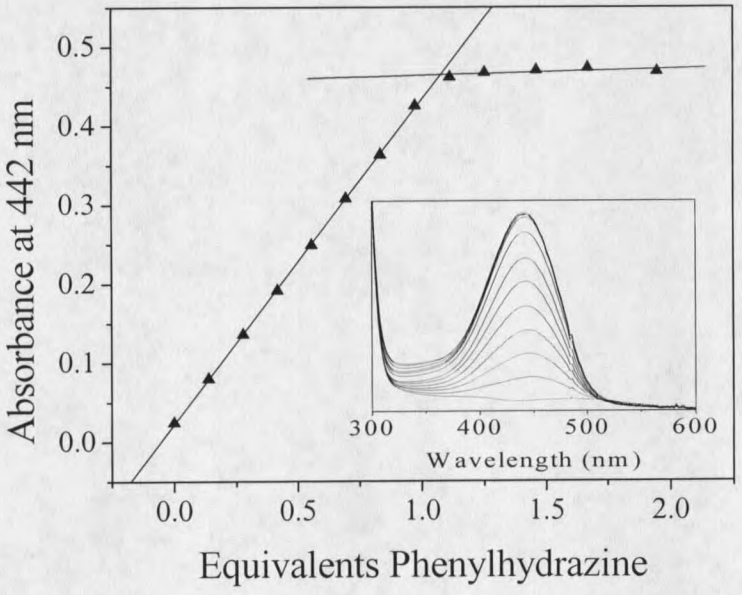

Figure 12. Phenylhydrazine titration of TPQ in purified rhKDAO. Plot shows the change in absorbance at 442 nm versus equivalents phenylhydrazine added per enzyme dimer. One mL of enzyme (11.8 μM enzyme in 100 mM potassium phosphate buffer, pH 7.2) titrated with 2 830 μM phenylhydrazine. The inset shows the increase in absorption of the intensely yellow-colored adduct with successive phenyhydrazine additions.

The resonance Raman spectrum of phenylhydrazine-derivatized recombinant enzyme is shown in Figure 13, along with that of the phenylhydrazone of TPQ-hydantoin, a model compound for the cofactor. Protein was concentrated after extensive buffer exchange to remove unreacted phenylhydrazine. The two spectra are essentially identical and thus conclusively identify TPQ as the quinone cofactor in the recombinant enzyme. Neither the visible absorption nor the resonance Raman spectrum of the phenylhydrazine adduct of rhKDAO suggests the visible absorption feature at ~400 nm reacts with this carbonyl reagent. Thus this unidentified absorption feature may be a modified form of the TPQ cofactor which is conformationally inaccessible to phenylhydrazine or one which is lacking a reactive carbonyl.

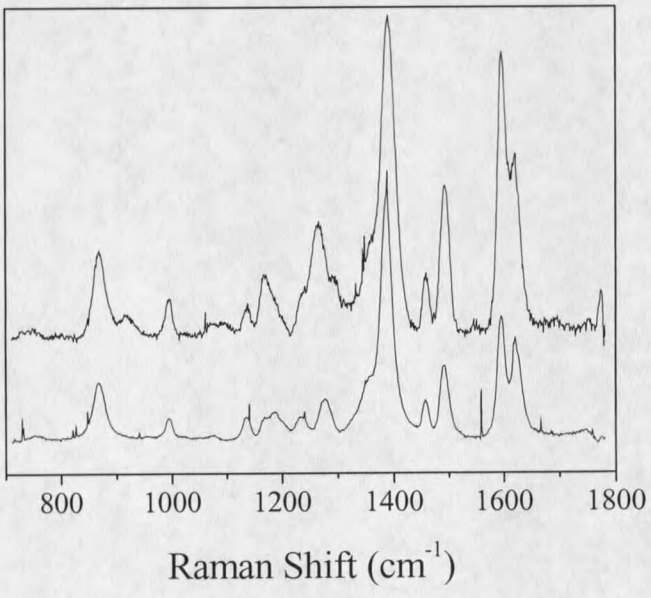

Figure 13. Resonance Raman spectra of the phenyhydrazine-derivatized human rhKDAO (upper spectrum). Lower spectrum is the phenylhydrazine-derivatized model compound, TPQ-hydantoin. Experimental conditions: excitation 457.9 nm, power 40 mW, integration 1 min, 10 accumulations.

Tissue-Specific Expression

A commercially available array of poly A^+ RNA representing 76 different human tissues and cell lines was probed with ^{35}P-labelled kidney diamine oxidase cDNA probes. The amount of poly A^+ RNA dotted on the nylon membrane were normalized by the manufacturer to give similar signal intensities for eight housekeeping genes and therefore varies from 53-780 ng. Each dot is 1 mm in diameter. Exposed and developed x-ray film is shown in Figure 14. Although the data are not quantifiable, a qualitative interpretation is informative for comparative analysis of tissue-specific gene expression. The highest levels of diamine oxidase gene expression are in placenta, followed by kidney tissue. Exposure at these two mRNA spots has clearly over-saturated the photographic media. Therefore actual mRNA levels may be orders of magnitude greater than that indicated by examination of the film. Gene expression is detectable in stomach tissue and quite significant through the distal tissues of the gastrointestinal tract. Prostate and liver also show fairly strong signals. A positive can be seen with *E. coli* DNA; however, kidney diamine oxidase cDNA and the bacterial genome have no significant sequence homology, and this is assumed to be a false positive. A similar false positive has previously been reported [47]. Low, but detectable, positive results are seen in stomach, bone marrow, lung, pancreas, testis, lymph node and the parietal lobe and pons of human brain. Negative results for controls other than the *E. coli* DNA, as well as for the majority of human tissues and cell lines, suggest that these are genuine positives. However, the weak results for these tissues, as compared to strong signals from other tissues, are such that actual gene expression levels in these tissues are normally quite low.

	1	2	3	4	5	6	7	8	9	10	11	12
A	whole brain	cerebellum, left	substantia nigra	heart	esophagus	colon, transverse	kidney	lung	liver	leukemia, HL-60	fetal brain	yeast total RNA
B	cerebral cortex	cerebellum, right	accumbens nucleus	aorta	stomach	colon, desending	skeletal muscle	placenta	pancreas	HeLa S3	fetal heart	yeast tRNA
C	frontal lobe	corpus callosum	thalamus	atrium, left	duodenum	rectum	spleen	bladder	adrenal gland	leukemia, K-562	fetal kidney	*E. coli* rRNA
D	parietal lobe	amygdala	pituitary gland	atrium, right	jejunum		thymus	uterus	thyroid gland	leukemia, MOLT-4	fetal liver	*E. coli* DNA
E	occipital lobe	caudate nucleus	spinal cord	ventricle, left	ileum		peripheral blood leukocyte	prostate	salivary gland	Burkitt's lymphoma, Raji	fetal spleen	Poly r(A)
F	temporal lobe	hippo-campus		ventricle, right	ilocecum		lymph node	testis	mammary gland	Burkitt's lymphoma, Daudi	fetal thymus	human C_0t -1 DNA
G	p.g.* of cerebral cortex	medulla oblongata		inter-ventricular septum	appendix		bone morrow	ovary		colorectal adeno-carcinoma, SW480	fetal lung	human DNA 100 ng
H	pons	putamen		apex of the heart	colon, ascending		trachea			lung carcinoma, A549		human DNA 500 ng

* paracentral gyrus

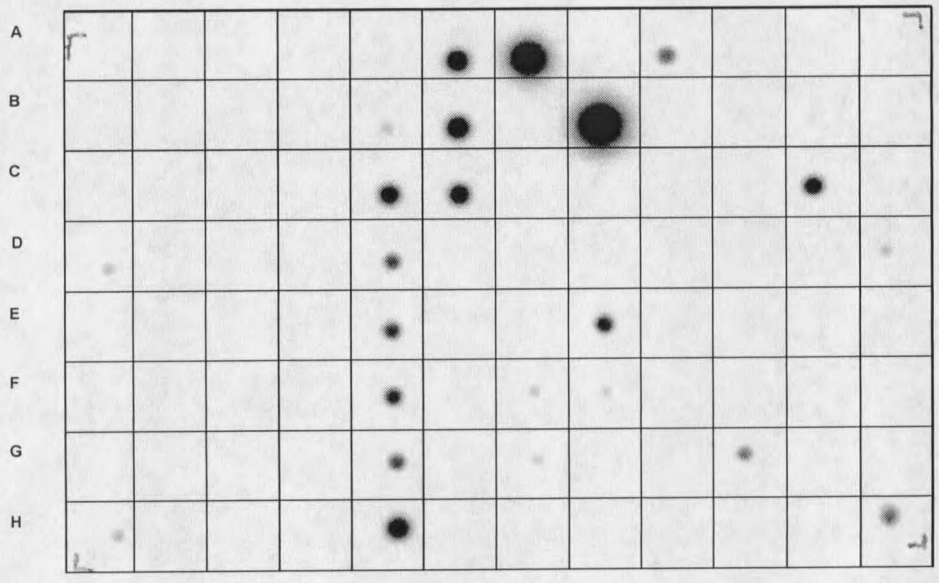

Figure 14. Multiple human tissue expression array with polyA mRNA from 76 tissues and cell lines (Clontech). Probed with randomly primed ^{32}P-labeled oligonucleotides generated by PCR from a cDNA clone of human kidney diamine oxidase.

Discussion

The gene encoding human kidney diamine oxidase, under the control of the metallothionein promoter, has been expressed in a *Drosophila* S2 polyclonal cell line. This work describes the first overexpression and purification of a copper-containing amine oxidase from any animal source. Expression levels for the secreted, recombinant enzyme are substantial, approaching 20 mg/L of cell culture. Almost certainly the abundant rhKDAO is a consequence of stably-transfected *Drosophila* S2 cell lines generally containing multicopy genomic inserts of the expression and selection plasmids, often with 500-1000 copies arranged in a head-to-tail fashion [48]. Very recently, Koyanagi and coworkers reported the heterologous overexpression of a copper amine oxidase from a multicellular organism, the plant *P. sativum* [49]. Unfortunately, low expression levels and considerable clonal variation mar this notable accomplishment (K. Tanizawa, pers. comm.). Expression of the *Arabidopsis thaliana* enzyme has previously been described in a baculovirus expression system [50].

Expression in serum-free media avoids introduction of exogenous copper amine oxidases [51,52] as well as the considerable amount of undesired proteins naturally present in fetal calf serum. Furthermore, searches of the *D. melanogaster* genome have not revealed any sequences with significant homology to CAOs, nor, to the best of our knowledge, has a CAO been described from any insect source. However, one member of the copper-containing amine oxidase family, lysyl oxidase (E.C. 1.4.3.13) has been identified in the *Drosophila* genome [53]. Lysyl oxidase contains a lysine-

tyrosylquinone cofactor and catalyzes the oxidative deamination of peptidyl lysine in elastin and collagen—a crucial step for connective tissue cross-linking [54]. Therefore the *Drosophila* Expression System, when used with serum-free media, is an excellent source of secreted human diamine oxidase, with the inherent advantages of low levels of unwanted proteins and apparently no contaminating CAOs, either exogenous or endogenous. *Drosophila* S2 cell have previously been used to express another copper enzyme, human dopamine β-hydroxylase, at protein yields quite similar to those reported in this work [55]. This expression system is thus a promising option for the convenient expression of other eukaryotic metalloenzymes.

Interestingly, in insects histamine is a major neurotransmitter. Histamine is a neurotransmitter in some mechanosensory neurons in *Drosophila*, lobster stomatogastric, cardiac, and olfactory neurons, and has recently been shown to be the major neruotransmitter in arthropod photoreceptors. [56-61]. It will be shown later that histamine is an excellent substrate for human KDAO. The mechanism for histamine catabolism in arthropods remains to be delineated, but a copper amine oxidase does not seem to be involved.

The natural hKDAO heparin-binding site facilitated the development of a rapid purification scheme resulting in the highly efficient recovery of greater than 99% homogenous recombinant human KDAO. The protein yields are impressive, approaching 20 mg/L.

Analytical ultracentrifugation results suggest rhKDAO contains between 20 and 26% glycosylation by weight, a value not unreasonable for the natural mammalian

enzyme. The results given by Crabbe et al. indicate approximately 40% glycosylation for the natural human placental enzyme [43]. Gel filtration by Baylin and Margolis suggest 20% glycosylation for the natural human pregnancy plasma DAO [44]. For comparison, the porcine kidney DAO has been estimated at 20% and 11% carbohydrate by weight [62,63]. Although the data on glycosylation in mammalian DAOs are limited—and it must be noted that differences in glycosylation could very well be tissue-specific—the extent of glycosylation by weight in rhKDAO is within the range of values reported for the natural enzymes.

SDS/PAGE and analytical ultracentrifugation results are consistent with a substantially glycosylated recombinant enzyme, as would be expected for a protein with potential glycosylation sites and processed through the secretory pathway. Electrospray mass spectrometry of the recombinant human kidney protein gave a large *m/z* "hump" with no resolvable peaks, indicative of a population of heterogeneously glycosylated proteins (data not shown). Four consensus N-glycosylation sequences (NXS/T) are present in the peptide sequence of human kidney diamine oxidase. N-linked glycosylation in *Drosophila* is much like that in other insect cells, with a high mannose content, although O-linked glycosylation is also possible[64,65]. Glycosylation of the recombinant enzyme is expected to be different from the enzymes processed in mammalian cells, and strategies to reduce the extent of glycosylation in rhKDAO are actively being pursued.

The heterologously expressed enzyme contains substoichiometric copper and displays some variability in copper levels from different purifications. The data shown in

Table 2 indicate copper content ranges from 1 to 1.5 ions per dimer. The recombinant enzyme most likely contains tightly bound zinc in the remaining active sites; copper and zinc together account for nearly full metal occupancy of the two active sites in each protein homodimer. Zinc has previously been described in recombinant *H. polymorpha* CAO overexpressed in *Saccharomyces cerevisiae*, and zinc was determined to have a high affinity for the active site and to compete with copper for binding [66]. The crystal structure of zinc-substituted *H. polymorpha* enzyme has recently been solved and reveals zinc in the active site, coordinated by three histidine residues and a tyrosine residue (copper ligands in the active enzyme and the tyrosine precursor of TPQ) [67]. These residues are remarkably similar in position as those described in the active site of apoCAO from *Arthrobacter globiformis* [13].

It is proposed that active-site metal incorporation most likely occurs intracellularly during rhKDAO processing in the Drosophila secretory pathway, and not following secretion into media loaded with 500 μM copper, in which case fully copper-loaded protein could be expected. Rae *et al.* have made a convincing argument for extraordinarily low levels of "free" intracellular copper, less than one per cell, and suggested copper-dependent enzymes require accessory factors (i.e. metallochaperones) [68]. However, their analysis is based upon *cytoplasmic* superoxide dismutase and would not necessarily apply to the contents of membrane bound organelles, such as those of the secretory pathway. Copper most likely enters the *Drosophila* secretory pathway via a P-type ATPase, homologous to the human Menkes disease protein, localized in the trans-Golgi network [69]. To date, no accessory protein for any CAO has been described.

Furthermore, *Drosophila* S2 culture is quite likely a zero background expression host and therefore would not be expected to possess a specific CAO metallochaperone. Copper and zinc content in the overexpressed enzyme may be determined by the total metal ion availability in the secretory pathway and the relative affinity of the active site for these two transition metals. Differences in metal loading between purifications might be the consequence of subtle and as yet unrecognized factors during cell culturing and protein expression.

This study indicates calcium occupies the putative second metal binding site in recombinant human kidney diamine oxidase. The high specificity and affinity of this site for calcium, supported by the resistance to removal by EDTA (log K = 10.61 at 25 °C [70]), strongly suggest calcium would be present in the natural enzyme. Stoichiometric calcium is also present in highly purified equine plasma copper amine oxidase (*vide infra*).

Although calcium sites in proteins vary considerably with regard to their coordination structure, the second-metal site in copper amine oxidases is unusual when compared to other structurally defined sites (see reference [71] for a recent review of the diverse calcium binding sites in proteins). Five putative KDAO calcium ligands can be deduced from sequence alignment and the crystal structures of the CAOs from *E. coli* and *P. sativum* [11,12]. Three of these are aspartyl carboxylates and the backbone carbonyl of a leucine in the sequence AspLeuAsp. These residues are located at the C-terminus of one β strand. The other two protein-derived oxygen donors are an aspartyl carboxylate and an adjacent backbone carbonyl (Leu), located at the N-terminus of another β strand.

Interestingly, the opposite ends of these two β strands (7-10 residues away) also provide the active site copper ligands. One coordinating water molecule is resolved in the crystal structures, giving an octahedral coordination geometry with calcium-oxygen distances from 2.2 to 2.5 Å (Figure 15).

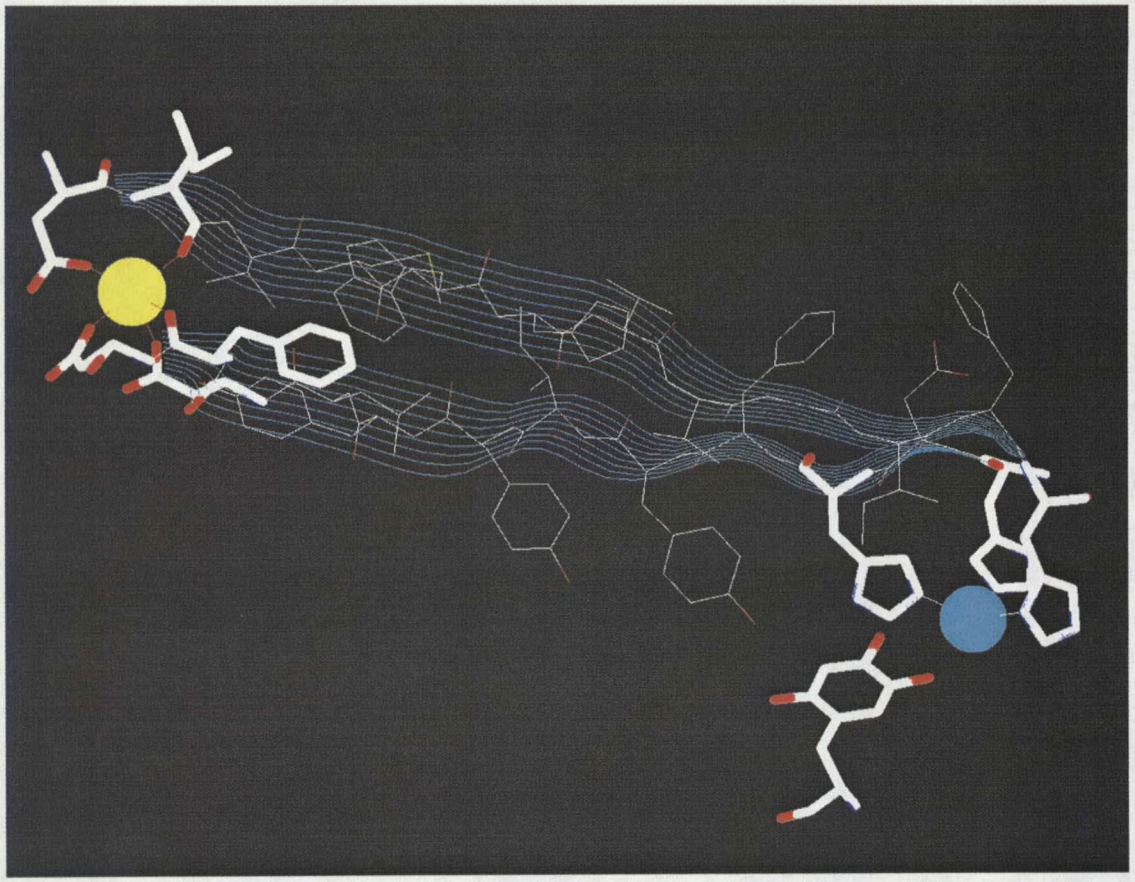

Figure 15. View of the copper and second metal binding sites from pea seedling amine oxidase. Copper is depicted as a cyan sphere and calcium as a yellow sphere. The protein residues that ligate the metal ions are shown in white with red representing oxygen atoms.

Most calcium ions in biology are heptacoordinate and associated with α helical and loop regions [72]. The well-known and extensive family of helix-loop-helix (EF hand) calcium sites is typically seven-coordinate with three carboxylates (one of which is

bidentate) two carbonyls, and one water molecule in a pentagonal bipyramid. EF hand ligands are all located in a short sequence at the end of one helix, a small loop, and the beginning of another helix. In contrast, the calcium binding residues in CAOs are at the ends of two β strands separated in sequence by more than 130 intervening amino acids.

Calcium ions are critical for a variety of important biological processes, including some involving extracellular proteins [73-78]. The function of the second metal site in copper-containing amine oxidases remains to be elucidated. However, the bound calcium ion likely serves to stabilize the structure of this extracellular enzyme, although a role in modulating activity is also possible but unlikely given the apparently high affinity for calcium and the separation between the putative Ca site and the active site.

Recombinant human kidney diamine oxidase is conclusively demonstrated to possess the TPQ cofactor. Visible absorption, CD, titration with phenylhydrazine, and resonance Raman of the phenylhydrazine-derivatized enzyme are entirely consistent with previously characterized copper amine oxidases from various sources [2,79]. Similar correlations between specific activity and titratable TPQ have been described by Klinman and coworkers for the bovine plasma amine oxidase and the recombinant yeast methylamine oxidase [35,80]. As shown in Table 2, the titratable TPQ from three different preparations is consistently around 72% of that which could be expected given the copper to protein stoichiometry, assuming that each active site containing copper would readily convert the precursor tyrosine to TPQ. It is presently unclear whether low TPQ-to-copper ratios reflect incomplete organic cofactor biogenesis or enzyme conformations in which the quinone cofactor is inaccessible to phenylhydrazine. Low

and variable TPQ content is not uncommon in CAOs [2]. For example, recombinant yeast methylamine oxidase has been described as containing 2.0 mol copper but only 1.5 mol phenylhydrazine-titratable TPQ per mol of enzyme dimer [80], a TPQ to copper ratio strikingly close to the results presented herein.

Conclusions

Human kidney diamine oxidase has been heterologously overexpressed in *Drosophila* S2 cell culture. The secreted enzyme is readily purified by three chromatography steps and gives high yields of essentially pure protein. This accomplishment provides the first example of a recombinant copper amine oxidase from any multicellular source. Although the enzyme does not contain a full complement of copper and TPQ, it has proven to be well suited to characterization and analysis.

Spectroscopic and biochemical analysis has clearly established that recombinant hKDAO contains the cofactors copper and TPQ. The visible absorption, CD, EPR and resonance Raman spectra of native rhKDAO as well as the visible and resonance Raman spectra of the phenylhydrazine-derivatized enzyme have been reported and are consistent with the data for copper amine oxidases from other sources.

The recombinant enzyme has only now allowed the detailed characterization of a human copper amine oxidase, a significant and long-awaited development in the field of copper amine oxidase research. Furthemore, biochemical and kinetic analysis, such as

the studies presented in the following chapters, provides key details required to reasonably infer the *in vivo* functions of diamine oxidase in human amine metabolism and homeostasis.

STEADY STATE KINETICS AND SUBSTRATE PREFERENCE OF rhKDAO

Introduction

A variety of biogenic and exogenous amines have been investigated as potential substrates for the recombinant human kidney diamine oxidase. Steady state kinetic parameters have been determined. These *in vitro* experiments are necessary to delineate the reactivity of rhKDAO and enable comparison with other copper amine oxidases. The quantity and quality of the recombinant protein has made such detailed and extensive studies feasible and substantially adds to the characterization of this human enzyme. Substrate specificity determined *in vitro* allow one to infer the *in vivo* substrates and by extension the possible roles of diamine oxidase in human physiology and its contribution to the complete scheme of amine metabolism and homeostasis.

The non physiological and exogenous aromatic amines benzylamine, β-phenethylamine and *p*-dimethylaminomethylbenzylamine (DAB) are commonly used *in vitro* substrates for copper amine oxidases[81,82]. Their corresponding product aldehydes absorb light in the ultraviolet region, enabling spectrophotometric detection and direct enzymatic assays.

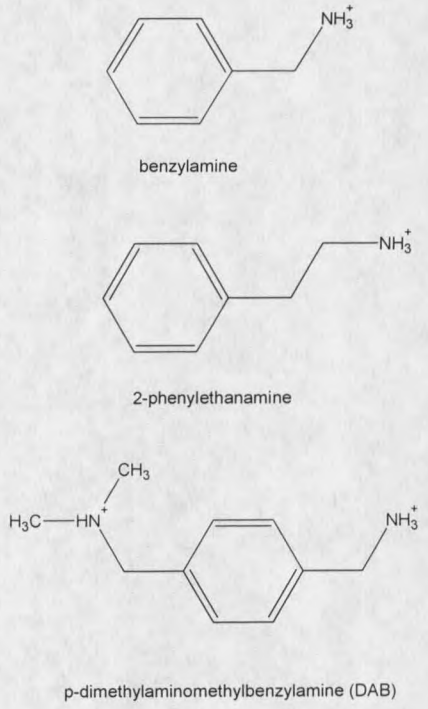

Figure 16. Structures of exogenous aromatic amine substrates for copper amine oxidases.

Figure 17 shows the structures of exogenous and endogenous aliphatic diamines and polyamines. Putrescine, cadaverine and the polyamines spermidine and spermine are widespread in biology and have been described as substrates for the copper containing diamine oxidases (*vide infra*).

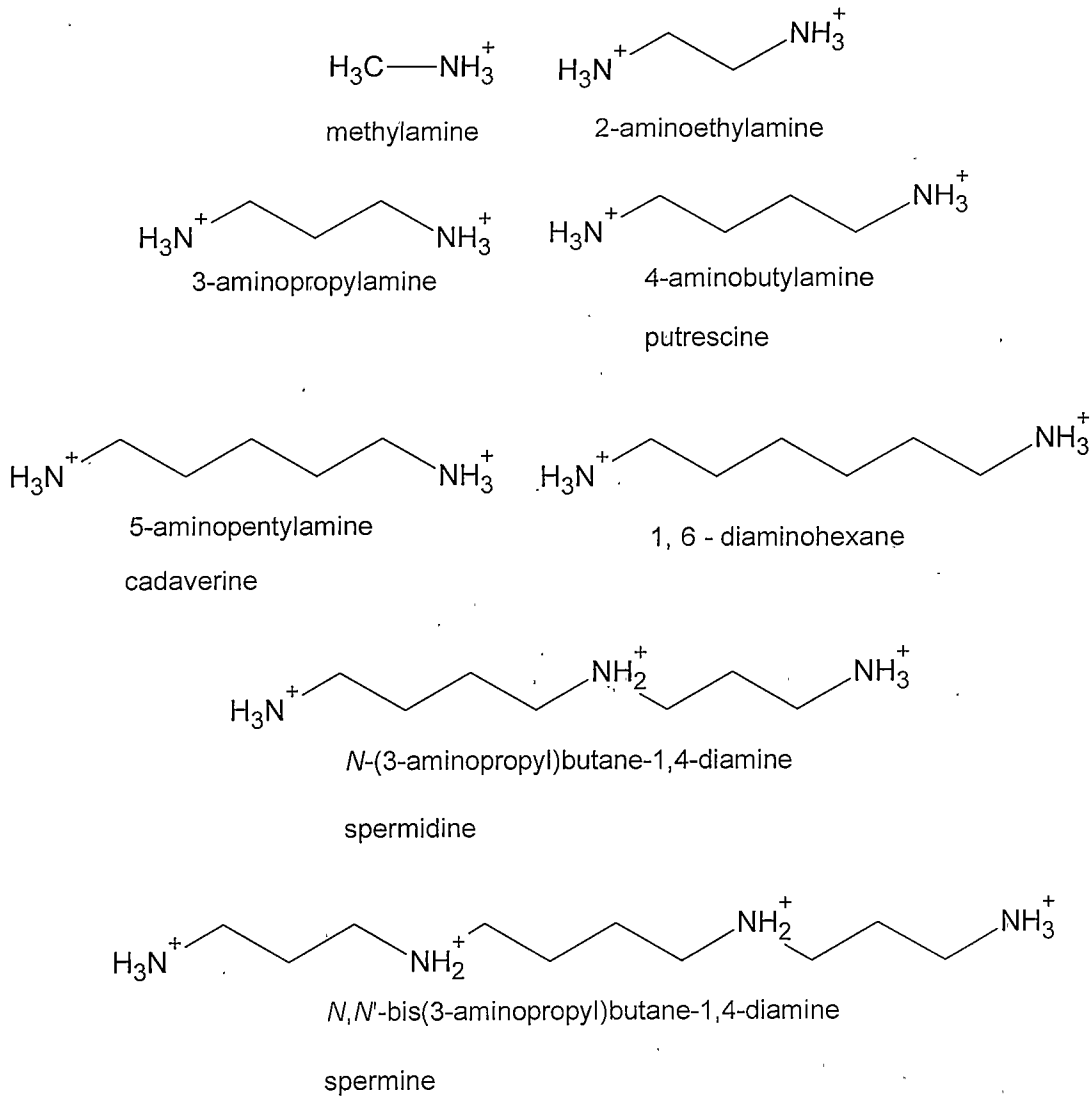

Figure 17. Structures of aliphatic diamines and polyamines

Histamine and 1-methylhistamine are metabolites of the amino acid histidine from decarboxylation and the subsequent methylation catalyzed by the enzymes histidine decarboxylase and histamine methyltransferase. Both are known substrates for mammalian diamine oxidases (*vida infra*). Histamine, in particular, is an extremely

potent biological agent acting as an agonist for G-protein coupled receptors and inducing a range of crucial physiological responses.

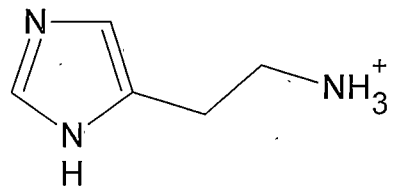

2-(1*H*-imidazol-5-yl)ethanamine

histamine

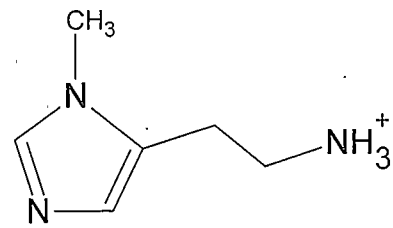

2-(1-methyl-1*H*-imidazol-5-yl)ethanamine

1-methylhistamine

Figure 18. Structures of histamine and 1-methylhistamine

Figure 19 shows the structure of the remaining compounds investigated as part of this study. Lysine and two ester derivatives were included in order to determine if this amino acid alone or as part of a peptidyl substrate could be a substrate for human DAO; in other words, to determine if diamine oxidase has a lysyl oxidase function. Metabolic derivates of the amino acids tryptophan, arginine and tyrosine were also included in this work.

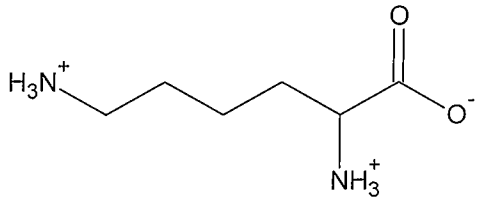

2,6-diaminohexanoate

L-Lysine

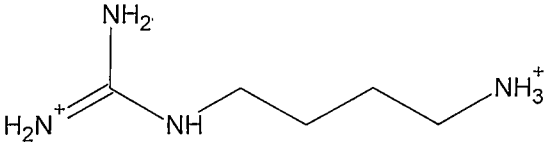

N-(4-aminobutyl)guanidine

agmatine

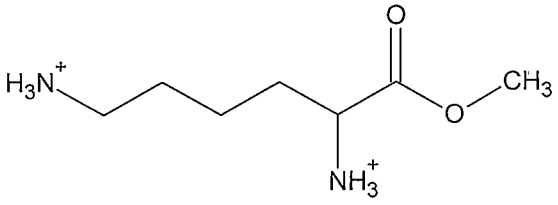

methyl 2,6-diaminohexanoate

L-Lysine methyl ester

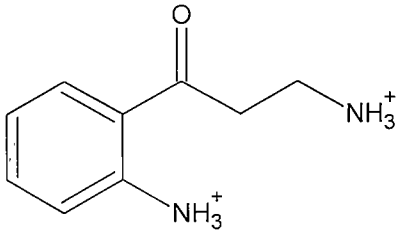

3-amino-1-(2-aminophenyl)propan-1-one

kynuramine

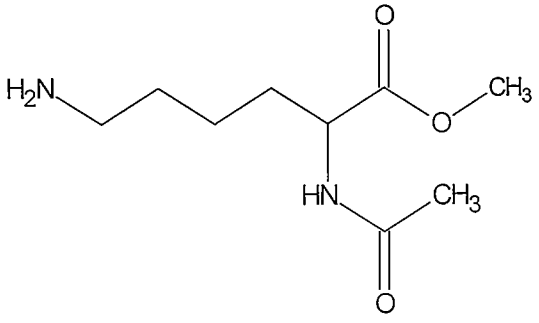

methyl 2-(acetylamino)-6-aminohexanoate

N-Acetyl-L-lysine methyl ester

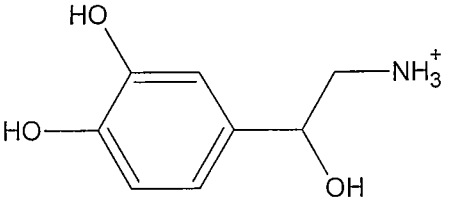

4-(2-amino-1-hydroxyethyl)benzene-1,2-diol

Arterenol (norepinephrine, noradrenaline)

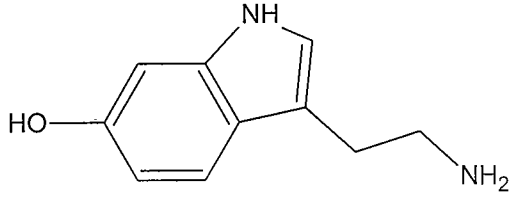

3-(2-aminoethyl)-1*H*-indol-6-ol

5-hydroxytryptamine (serotonin)

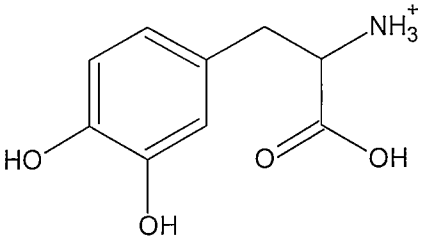

2-amino-3-(3,4-dihydroxyphenyl)propanoic acid

3-hydroxytyramine (dopamine)

Figure 19. Structures of derivatives of the amino acids lysine, arginine and tyrosine

Experimental Procedures

K_M and k_{cat} were determined spectrophotometrically in a 37 °C thermostatted cell holder with magnetic stirring. Ionic strength of the assay buffer, 50 mM HEPES, pH 7.2, was maintained at 150 mM by addition of potassium chloride. Oxidation of *p*-dimethylaminomethylbenzylamine (DAB) and benzylamine were followed by the change in absorbance at 250 nm, using an extinction coefficient of 11 $mM^{-1}cm^{-1}$ for *p*-dimethylaminomethylbenzaldehyde [82]. Assays with DAB or benzylamine used 890 µL of assay buffer and 10 uL enzyme in a 1 cm pathlength cuvette. This mixture was allowed to equilibrate for a 2-3 minutes in the thermostatted cell holder before rapid addition of 100 µL substrate stock solution. Data acquisition was initiated immediately. All other assays used the coupled assay of Holt et al. [83] and an extinction coefficient for the quinoneimine dye of 6.00 $mM^{-1}cm^{-1}$ at 498 nm [84]. Chromogen stock solution was prepared to give final concentrations of 1 mM 4-aminoantipyrine and 2 mM vanillic acid. Coupled assays used 880 µL chromogen stock solution, 10 µL (14.5 U) horseradish peroxidase, and 10 µL enzyme. Substrate, horseradish peroxidase and chromogen stock solutions were freshly prepared in the assay buffer, and kept in a 37 °C water bath until use. Recombinant diamine oxidase was kept on ice. Thermal equilibration, substrate addition and data acquisition were as described above. Assays used 10 µL of 4.37 µM recombinant human kidney diamine oxidase, except 4.09 µM enzyme with 1-methylhistamine, and 4.67 µM with putrescine and agmatine. Water bath and thermostatted cell holder temperatures were monitored with an electronic thermocouple.

Initial rates were determined by at least duplicate experiments (most often triplicate) at six or more substrate concentrations with fitting to the Michaelis-Menten equation using Origin 6.0 software (OriginLab Corp.). Those substrates demonstrating substrate inhibition were fit as described below [85]:

(a) Substrates that indicated hyperbolic behavior were fit with the Michaelis-Menten equation:

$$v = \frac{S\ V_{max}}{S + K_M}$$

(b) Where required fits used a simple model of substrate inhibition:

$$v = \frac{S\ V_{max}}{\frac{S^2}{K_i} + K_m + S}$$

(c) In a few cases the fits to data used the following equation, for a model with reversible substrate inhibition at two different forms of the enzyme:

$$v = \frac{S\ V_{ma}}{K_3 S2 + S + K_2 S + K_1}$$

Figure 20 shows the schematics for the models that represent the kinetic equations above. Appendix C gives detailed information on the derivation of these equations.

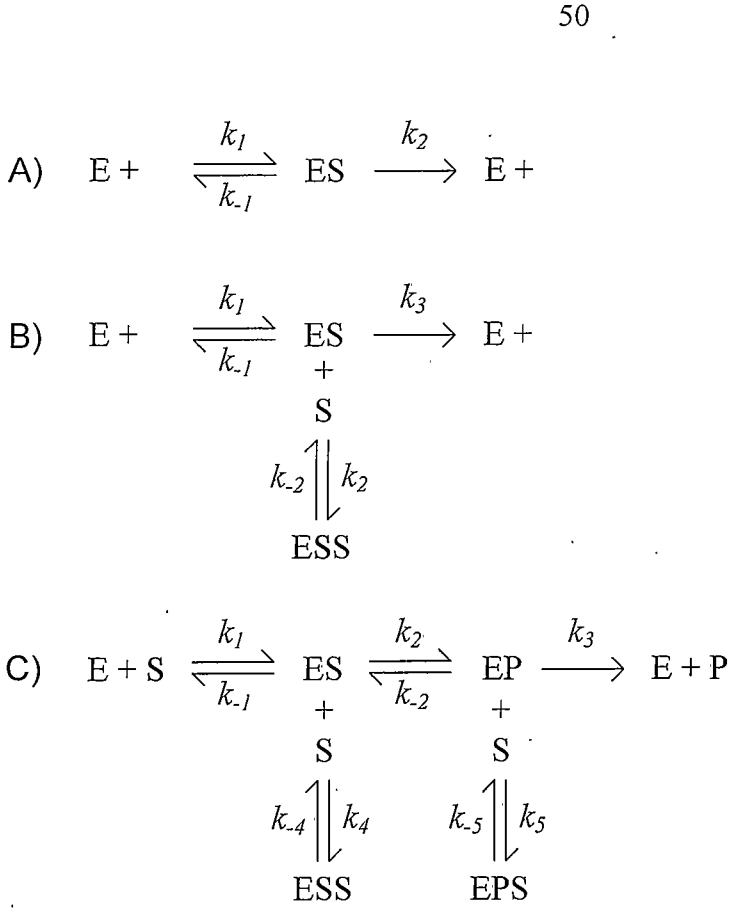

Figure 20. Mechanistic models used to derive enzyme rate equations: **A)** Michaelis-Menten model; **B)** Substrate inhibition; **C)** Substrate inhibition at two enzyme states

Substrates that oxidized either extremely slowly or at rates undetectable under these conditions were assayed up to millimolar substrate concentrations. Potential substrates were purchased commercially (highest grade available) and used without further purification, except for DAB, which was synthesized by the method of Bardsley et al. [82].

The pH dependence of Michaelis-Menten parameters for the oxidation of putrescine was determined using the coupled 4-aminoantipyrine/vanillic acid assay as described above. Buffers used were 50 mM MES (pH 5.69 - 6.33), 50 mM HEPES (pH

6.33 - 7.78), and 50 mM CHES (pH 8.12 and 8.85). Ionic strength was adjusted to a final concentration of 150 mM with potassium chloride. After equilibration at 37 °C, the pH was measured with an Orion perpHect LogR meter, model 310, equipped with an Automatic Temperature Compensation Probe. At least two (usually three or four) initial rates were determined at six or more substrate concentrations for each pH value. k_{cat} values were plotted against proton concentration and fit to the following equation [86]:

$$k_{cat} = (k_{cat})_{max}[H^+]K_{a1} / (K_{a1} K_{a2} + K_{a1} [H^+] + [H^+]^2)$$

Enzyme stability in the pH range used was tested by incubation of enzyme in the appropriate buffers for 15 minutes at 37 °C and then measuring activity. Possible effects of pH on the quinoleimine dye generated during the assay were investigated by titrating hydrogen peroxide into the chromogenic solution plus horseradish peroxidase at appropriate pH values. Neither loss of enzyme activity nor change in quinoleimine dye absorption features was detected in the buffers and pH range investigated.

Heparin effects on enzyme activity were investigated by incubating recombinant kidney diamine oxidase with an approximately four-fold excess of heparin (from porcine intestinal mucosa, average molecular weight of 3,000 Da, Sigma) over dimeric protein for one hour on ice. Initial rate determinations for putrescine oxidation were as described above. The enzyme-heparin mix was stored at 4 °C and assayed for activity with 250 μM putrescine after 24, 48, and 72 hours. All assays used air saturated solutions and dissolved oxygen levels were not varied in these experiments (about 233 μM).

Results

The data and fits to the data are given in Figures 21 - 34. The results are summarized in Table 3 and are listed in order of the substrate preference of rhKDAO indicated by k_{cat}/K_M.

The data for histamine turnover clearly indicate partial substrate inhibition. The fit using the model of substrate inhibition required masking of the data points at higher concentrations of histamine, and as shown this model is inadequate for completely describing the data (Figure 21). A model with substrate inhibition at two forms of the enzyme was also fit to the data, and shown in Figure 22. This model also proved inadequate and required masking of the data for the higher concentrations of histamine. Note that the apparent K_M and V_{max} values for both of these models are approximately equal and that the fit curves have identical shapes.

It became apparent that no model of partial substrate inhibition would fit all the data points; partial substrate inhibition alone cannot account for the data points at the higher concentrations of histamine. A model that can fit all the data requires an additional mechanism for substrate oxidation, a process that becomes evident at higher substrate concentrations. The data were accordingly fit to the model for substrate inhibition plus an additional Michaelis-Menten model, that is:

$$v = \frac{S V_{max}}{\frac{S^2}{K_i} + K_m + S} + \frac{S V_{max}}{S + K_M}$$

Figure 23 shows that this kinetic model can be used to reasonably fit all the data points.

Compound	K_M (μM)	k_{cat} (min^{-1})	k_{cat}/K_M ($\mu M^{-1} min^{-1}$)
Histamine[c]	3.4 ± 0.08	159 ± 1.1	47
1-Methylhistamine	3.0 ±0.1	100 ± 1.0	33
Agmatine[c]	13 ± 1.0	324 ± 17	25
Putrescine[c]	17 ± 0.5	329 ± 3.1	20
Cadaverine	22 ± 0.3	411 ± 4.1	19
DAB	113 ± 2	532 ± 5.3	4.7
1,3 - Diaminopropane	129 ± 14	486 ± 22	3.8
1,6 – Diaminohexane	177 ± 12	324 ± 9	1.8
2-aminoethylamine	626 ± 11	127 ± 0.6	0.2
Spermidine	1092 ± 8.3	187 ± 0.5	0.2
L - Lysine methyl ester	2978 ± 114	346 ± 4.6	0.1
(–) – Arterenol	+[a]	+	+
Benzylamine	+	+	+
3 – Hydroxytyramine	+	+	+
Kynuramine	+	+	+
β-Phenethylamine	+	+	+
Spermine	+	+	+
5 - Hydroxytryptamine	-[b]	-	-
L- Lysine	-	-	-
Nα-acetyl-L-lysine methyl ester	-	-	-
Methylamine	-	-	-

Table 3. Steady-state kinetic parameters and substrate specificity (k_{cat}/K_M) for recombinant human kidney diamine oxidase. Errors are reported as standard error at the 95% confidence level. Partial substrate inhibition was observed with histamine, agmatine and putrescine.

a The positive symbol (+) denotes substrate oxidation could be detected but at rates too low to determine kinetic parameters.

[b] The negative symbol (-) indicates no rate was observed.

[c] Partial substrate inhibition was observed.

Fits to the more complex model increases the error in each fit parameter. Therefore to derive apparent K_M and V_{max} values the data were fit to the substrate inhibition model with the data points at high substrate concentrations disregarded. The data for agmatine oxidation were also interpreted in this manner.

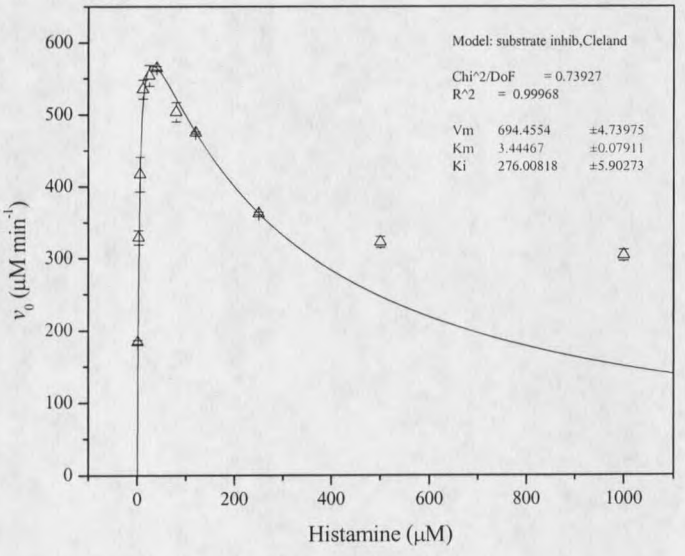

Figure 21. Histamine, fit to the substrate inhibition model

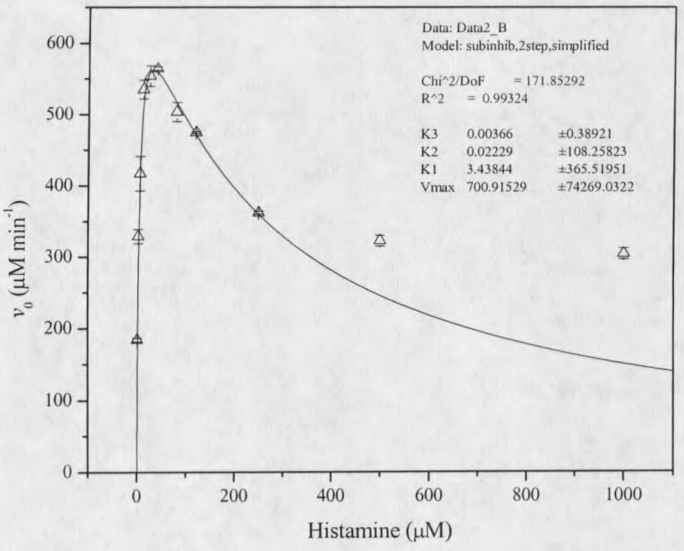

Figure 22. Histamine fit to the substrate inhibition at two enzyme forms

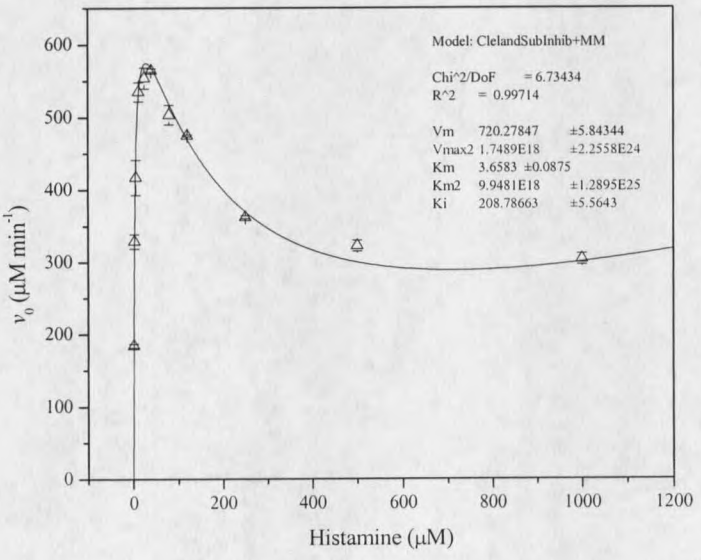

Figure 23. Histamine fit to the substrate inhibition model plus an additional Michaelis-Menten model

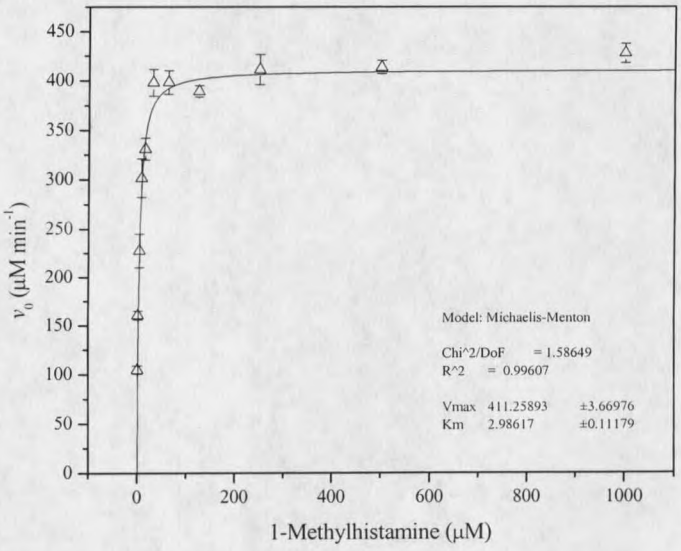

Figure 24. 1-methylhistamine fit to the Michaelis-Menten model

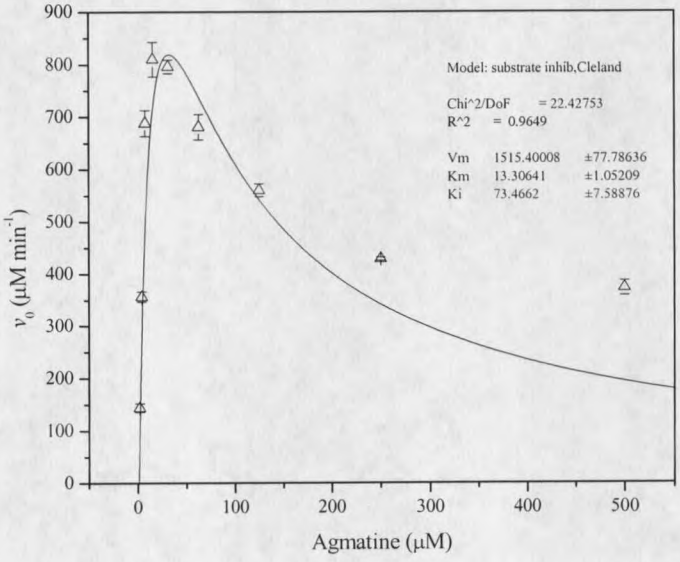

Figure 25. Agmatine fit to the substrate inhibition model

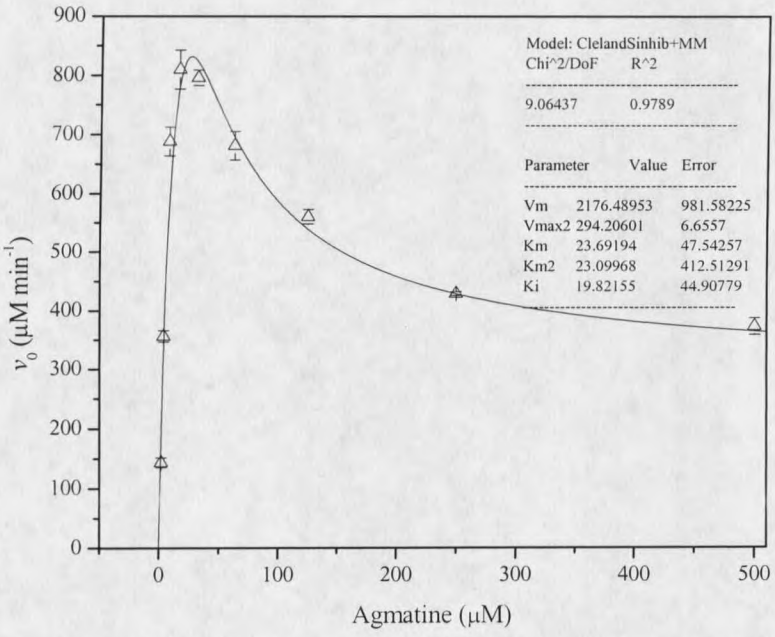

Figure 26: Agmatine fit to the substrate inhibition model plus an additional Michaelis-Menten model.

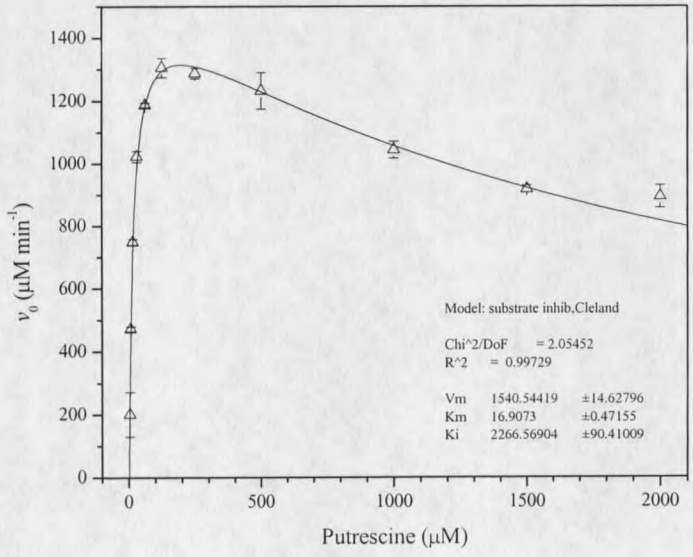

Figure 27. Putrescine fit to the substrate inhibition model

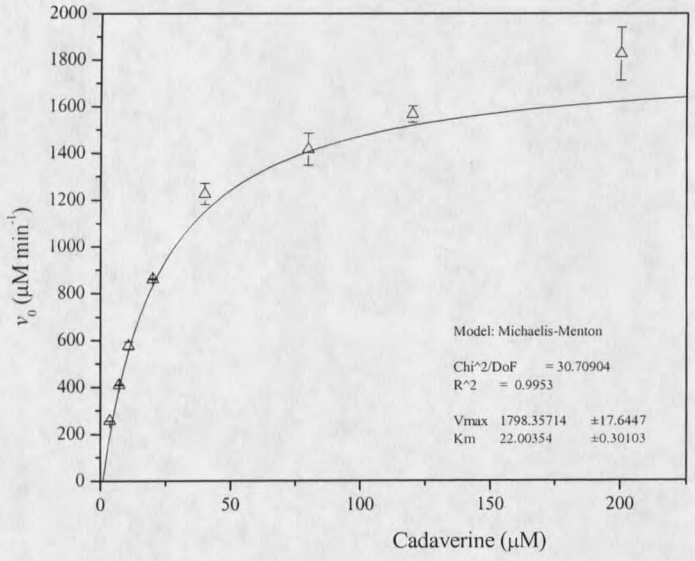

Figure 28. Cadaverine fit to the Michaelis-Menten model

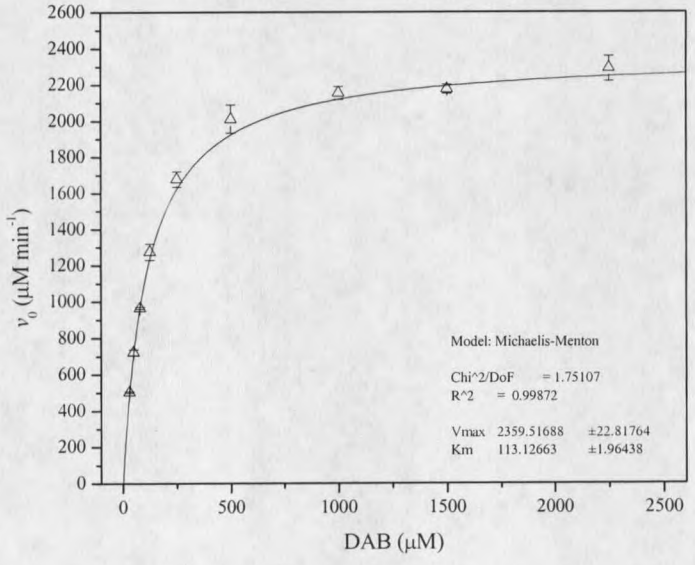

Figure 29. DAB fit to the Michaelis-Menten equation